JGR Biogeosciences

RESEARCH ARTICLE
10.1029/2019JG005500

Special Section:
The Energy Exascale Earth System Model (E3SM)

The Central Amazon Biomass Sink Under Current and Future Atmospheric CO_2: Predictions From Big-Leaf and Demographic Vegetation Models

Jennifer A. Holm[1], Ryan G. Knox[1], Qing Zhu[1], Rosie A. Fisher[2,3], Charles D. Koven[1], Adriano J. Nogueira Lima[4], William J. Riley[1], Marcos Longo[5,6], Robinson I. Negrón-Juárez[1], Alessandro C. de Araujo[7], Lara M. Kueppers[1,8], Paul R. Moorcroft[9], Niro Higuchi[4], and Jeffrey Q. Chambers[1,8]

[1]Lawrence Berkeley National Laboratory, Berkeley, CA, USA, [2]National Center for Atmospheric Research, Boulder, CO, USA, [3]Centre Européen Research et de Formation Avencée en Calcul Scientifique (CERFACS), Toulouse, France, [4]Instituto Nacional de Pesquisas da Amazônia, Manaus, Brazil, [5]Embrapa Agricultural Informatics, Campinas, Brazil, [6]Jet Propulsion Laboratory, California Institute of Technology, Pasadena, CA, USA, [7]Brazilian Agricultural Research Corporation - Embrapa, Brasilia, Brazil, [8]Department of Geography, University of California Berkeley, Berkeley, CA, USA, [9]Department of Organismic and Evolutionary Biology, Harvard University, Cambridge, MA, USA

Abstract There is large uncertainty whether Amazon forests will remain a carbon sink as atmospheric CO_2 increases. Hence, we simulated an old-growth tropical forest using six versions of four terrestrial models differing in scale of vegetation structure and representation of biogeochemical (BGC) cycling, all driven with CO_2 forcing from the preindustrial period to 2100. The models were benchmarked against tree inventory and eddy covariance data from a Brazilian site for present-day predictions. All models predicted positive vegetation growth that outpaced mortality, leading to continual increases in present-day biomass accumulation. Notably, the two vegetation demographic models (VDMs) (ED2 and ELM-FATES) always predicted positive stem diameter growth in all size classes. The field data, however, indicated that a quarter of canopy trees didn't grow over the 15-year period, and while high interannual variation existed, biomass change was near neutral. With a doubling of CO_2, three of the four models predicted an appreciable biomass sink (0.77 to 1.24 Mg ha^{-1} year^{-1}). ELMv1-ECA, the only model used here that includes phosphorus constraints, predicted the lowest biomass sink relative to initial biomass stocks (+21%), lower than the other BGC model, CLM5 (+48%). Models projections differed primarily through variations in nutrient constraints, then carbon allocation, initial biomass, and density-dependent mortality. The VDM's performance was similar or better than the BGC models run in carbon-only mode, suggesting that nutrient competition in VDMs will improve predictions. We demonstrate that VDMs are comparable to nondemographic (i.e., "big-leaf") models but also include finer scale demography and competition that can be evaluated against field observations.

Key Points:
- We evaluate four terrestrial models, some in multiple versions, against a 15-year dataset of forest dynamics in Brazil
- Annual biomass increments from models were within field data uncertainty, but over 15 years large biomass accumulations emerged, inconsistent with field data
- With elevating CO_2 out to 2100, carbon-only models predicted large sinks, demography reduced this sink, and the model with phosphorus constraints predicted a substantially lower sink

Supporting Information:
- Supporting Information S1

Correspondence to:
J. A. Holm,
jaholm@lbl.gov

Citation:
Holm, J. A., Knox, R. G., Zhu, Q., Fisher, R. A., Koven, C. D., Nogueira Lima, A. J., et al. (2020). The central Amazon biomass sink under current and future atmospheric CO_2: Predictions from big-leaf and demographic vegetation models. *Journal of Geophysical Research: Biogeosciences*, *125*, e2019JG005500. https://doi.org/10.1029/2019JG005500

Received 5 OCT 2019
Accepted 23 JAN 2020
Accepted article online 28 JAN 2020

1. Introduction

The effects of rising atmospheric CO_2 concentrations on tropical forests have been the focus of a large body of research, and the question of whether intact tropical forests will act as a large CO_2 sink remains contested. Evidence supporting a sink includes a sequence of pantropical inventory analyses, which have suggested that the Earth's intact tropical forests sequester carbon at 1.4 Mg ha^{-1} year^{-1} globally, or roughly half of the global net terrestrial sink (Baker et al., 2004; Lewis et al., 2009; Pan et al., 2011; Phillips et al., 2008; Phillips et al., 1998). Evidence that is not in support of a large tropical carbon sink includes data from growth rings and stable carbon isotopes at tropical sites in South America, Africa, and Asia, which show no acceleration of individual tree growth over the past 150 years with historical CO_2 fertilization (van der Sleen et al., 2015). A 12-year field-based estimate found that the annual productivity of a tropical forest in Costa Rica did not increase as expected with elevating CO_2 (eCO_2), due to climatic stress (increasing minimum temperatures and greater dry-season water limitation) (Clark et al., 2013). Analysis of mature Amazonian forests suggests that the biomass sink may be declining in magnitude over the past two decades, a trend attributed primarily to increased mortality rates and a shift to faster life-history strategies (Brienen et al., 2015). A challenge with individual plot studies is the bias arising from underestimates of tree mortality from

rare, sporadic, small, and large disturbances, yet accurate individual tree growth estimates, yielding overestimation of net carbon sequestration (Körner, 2003). As Clark et al. (2017) and Wright (2013) point out, estimates of pantropical net carbon fluxes are uncertain and need better observational constraints.

Manipulative field experiments such as free-air CO_2 enrichment (FACE) studies provide needed insight on tree ecophysiology (Medlyn et al., 2015; Norby et al., 2010) and offer promise to fill knowledge gaps. A FACE experiment in the tropics is planned for the future and highly needed (Norby et al., 2016). To inform the experimental design needs of this upcoming AmazonFACE study, an ensemble of 14 ecosystem models showed that modeled phosphorus (P) feedbacks reduce the biomass sink by 50% compared to estimates from the carbon and carbon-nitrogen models (Fleischer et al., 2019). These experiments are on the order of one decade, and hence, do not capture progressive nutrient limitation effects or changes in forest functional composition. Quantification of the tropical forest carbon sink is also a grand challenge of measurement scale, and difficult to capture in FACE experiments, due to the geography of disturbance (Asner, 2013), and scaling from plot to continental scale introduces significant uncertainty that is difficult to quantify (Chambers et al., 2013).

There is large model uncertainty in plant responses to eCO_2 in Earth system models (ESMs) (De Kauwe et al., 2014; Ghimire et al., 2016; Hoffman et al., 2014; Zaehle et al., 2014), with key model algorithms that lead to divergent projections of carbon sequestration pertaining to plant nitrogen (N) uptake and stoichiometry, carbon (C) allocation to plant tissues, and self-thinning (Walker et al., 2015). Models participating in the Coupled Model Intercomparison Project 5 (CMIP5) (Taylor et al., 2012) estimate a wide range of net land carbon fluxes over the next century, including differences even in the sign of the flux (Friedlingstein et al., 2014), with estimates from tropical forests contributing to a large portion of the uncertainty. Apart from modeled land-use change assumptions contributing to the large spread among CMIP5 models, additional variability manifested in either the coupling of nutrients between soil and vegetation, gross primary productivity (GPP) responses to changes in CO_2 concentration, how assimilated carbon is allocated across biomass pools with different turnover periods, and variable carbon storage and flux in coarse woody debris and soil C (Luo et al., 2006; Medlyn et al., 2015; Thompson et al., 1996). In contrast to the more recent observational studies listed above, some global land surface models predict that tropical forests will act as a large, long-term C sink under eCO_2 (Huntingford et al., 2013; Rammig et al., 2010; Zhang et al., 2015).

1.1. Variations in Terrestrial Biosphere Model Approaches

Vegetation representation and ecosystem processes differ substantially across models, contributing to a large spread in ecological predictions. Therefore, we compare and evaluate examples of this spread using six versions of four terrestrial biosphere models that vary in their scale of representing vegetation structure, inclusion of demography, and plant nutrient competition (Table 1). We perform a quasi-factorial design to test structured vegetation dynamics and plant competition for nutrients as two critical processes to tropical forest dynamics and CO_2 fertilization responses (Figure 1), also referred to as direct "CO_2 effect" (i.e., β response). We begin with two biogeochemical models that simulate aggregated, coarse vegetation structure (i.e., "big-leaf" models), and therefore, do not represent dynamic vegetation processes in this study. As a baseline, we then applied these two models in their nutrient-unconstrained (i.e., C only) modes. After which we investigate the β response using these same two models with prognostic biogeochemical cycling and nutrient limitation. These two models are the Community Land Model version 5 (CLM5) (Lawrence et al., 2019; Oleson et al., 2013) and the Energy Exascale Earth System Model (E3SM) Land Model version 1.1 (ELMv1) with Equilibrium Chemistry Approximation (ECA) kinetics (Zhu et al., 2017) (ELMv1-ECA), with ELMv1 being based upon CLM4.5.

In contrast to the aggregated "big-leaf" approach, vegetation demographic models' (VDMs; Fisher et al., 2018) represents vegetation in a more highly resolved manner through demography. Cohorts of trees are distinguished by plant functional type, size structure, and age since disturbance, each competing in different growth phases which can be informed directly by field observations. For each cohort the dynamic process of recruitment, growth, and mortality is mechanistically represented and emergent properties due to competition. As a last test in the quasi-factorial design, we tested the β response in two VDMs, which here does not include nutrient limitation. Demography provides different sensitivities to eCO_2 via finer scale ecological

Table 1
Summary and Description of Relevant Model Processes, State Variables, and Key Parameters Found in ED2, ELM-FATES, CLM5, and ELMv1-ECA

	ED2	ELM-FATES	CLM5	ELMv1-ECA
Time step	15 min[a]	30 min[a]	30 min	30 min
Scale of vegetation	Gap scale	Gap scale	100 km^2	100 km^2
Dynamic vegetation	Yes	Yes	No	No
Biomass pools	L, WS, WH, R, ST, S	L, WS, WH, CR (L and D), FR, ST, S	L, WS, WH, CR (L and D), FR, ST, G	L, WS, WH, CR (L and D), FR, ST
Litter C pools	2	4	3	4
Soil C pools	3	3	3	3
C allocation	Pipe model, resource capture, allometric equations	Pipe model, resource capture, allometric equations	Fixed fractions	Flexible, dynamic based on light, nutrients, water stress
Mortality	Prognosed; five forms	Prognosed; five forms	Fixed annual mortality (2%)	Fixed annual mortality (2%)
LAI	Prognosed allometrically	Prognosed allometrically and via optimization	Prognostic based on C, N pools	Prognostic based on C, N pools
Photosynthesis	Collatz et al. (1991)	Farquhar et al. (1980)	Farquhar et al. (1980)	Farquhar et al. (1980)
Tissue stoichiometry	Fixed C:N ratios	Fixed C:N ratios	Flexible with target C:N ratio	Flexible stoichiometry
V_{cmax} ($\mu mol\ m^{-2}\ s^{-1}$)	Phenomenological thermal cutoff at very low and high temperatures	Fixed; 45	Prognostic via leaf utilization of N for assimilation	Prognostically calculated with leaf-level N and P content
Nutrient limitation of CO_2 fertilization	No	No	Yes	Yes
N cycle	Tracks leaf N mass balance[b]	No	Yes	Yes
P cycle	No	No	No	Yes

Note. Adopting terminology and abbreviations from Walker et al. (2014).
Abbreviations: L = leaf; WS = sapwood; WH = heartwood; R = roots; CR = coarse roots; FR = fine roots; ST = storage; S = seeds; L = live; D = dead; G = grain; CWD = coarse woody debris; C = carbon.
[a]Vegetation dynamics occur once per day. [b]N does not limit photosynthesis in this version.

processes, ultimately altering responses of land-atmosphere interactions (Levine et al., 2016; Purves & Pacala, 2008), which cannot be achieved in models with more aggregated vegetation.

The two VDMs used here are the Ecosystem Demography model 2.2 (ED2) (Knox, 2012; Longo, 2014; Medvigy et al., 2009), and the newly developed Functionally Assembled Terrestrial Ecosystem Simulator coupled to the global biophysical E3SM Land Model (ELM-FATES) (Fisher et al., 2015) both which simulate terrestrial ecosystems using physically based parameterizations of ecosystem processes. In previous model analyses over the Amazon Basin, Zhang et al. (2015) and de Almeida Castanho et al. (2016) both concluded that the ED2 model, when compared to two other terrestrial biosphere models (JULES and IBIS), exhibited the strongest "CO_2 fertilization" effect on vegetation productivity and sustained high tropical biomass. The version of ED2 used here does not represent nutrient constraints on productivity although evidence for downregulation of photosynthesis under eCO_2 is strong in experimental studies (Luo et al., 2004; McGuire et al., 1995; Medlyn et al., 1999).

1.2. Goal and Hypotheses

The goal of this study is to compare predictions of four terrestrial biosphere models with alternate representations of vegetation structure, demography, and nutrient biogeochemistry to present-day observations and to each other over an idealized long-term eCO_2 scenario.

Specifically, we compare the models to (i) a detailed 15-year field inventory dataset of present-day biomass, forest dynamics, and energy-water fluxes of an old-growth central Amazonian lowland forest. The site differs from typical single-site inventory plots, in that sampling occurred along long transects with undulating topography of plateau, slope, and valleys, and soil types more representatively, and thus provide a diverse landscape-scale estimate of forest dynamics. Next we compare (ii) the models to each other in simulating forest biomass responses to continuously rising atmospheric CO_2 concentrations out to 2100, and (iii) the critical processes across all models that influence the range and magnitude of potential biomass accumulation given varying constraints and model assumptions. Apart from de Almeida Castanho et al.

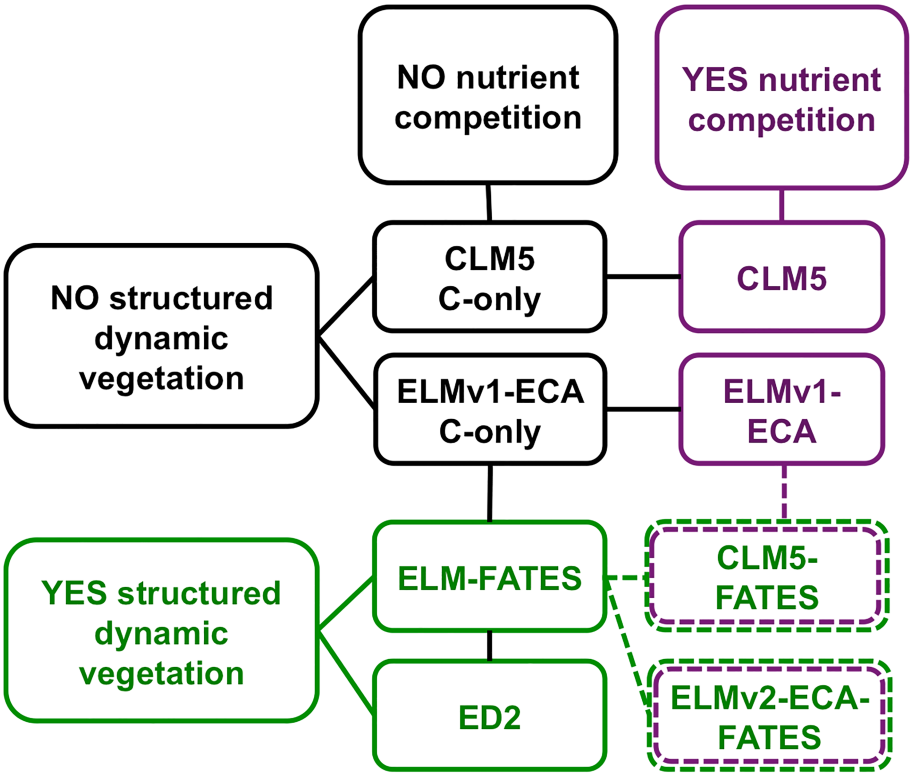

Figure 1. Quasi-factorial design for model comparison, showing the baseline case of two models with no structured dynamic vegetation and no plant or soil nutrient constraints (i.e., CLM5 and ELMv1-ECA big-leaf models run in C-only mode; black boxes and lines) and models with structure dynamic vegetation (ED2, ELM-FATES; green boxes and lines) or nutrient competition (CLM5, ELMv1-ECA; purple boxes and lines). The next release versions of the host land models will contain both dynamic vegetation via FATES and plant nutrient competition indicated by dashed lines.

(2016), there has been little evaluation of terrestrial models' abilities to simulate tropical biomass dynamics against field measurements with repeated inventories, distinguishing this study from others. The four models we apply here collectively span a range of vegetation structure scales, turnover dynamics, and nutrient cycling representations (with ELMv1-ECA being the only model considering P interactions). Further, this study takes a first step at comparing advantages or disadvantages of coupling a VDM to an ESM's land surface model by comparing ED2 and ELM-FATES outputs against observational data, relevant literature, and theory.

We test the hypothesis that the VDMs, which here, all lack nutrient dynamics and are parameterized for a generic Amazon forest, will better capture observed forest structure and dynamics over the inventory period and produce similar response to eCO_2 as the big-leaf C-only version, but larger positive response to eCO_2 when compared to the big-leaf nutrient-enabled vegetation models, due to nutrient limitations on plant growth. We also analyze the nutrient-enabled big-leaf models' predictions of increased N and/or P uptake through shifts in C allocation (represented in ELMv1-ECA only) and flexibility in plant C to nutrient ratios (as discussed as critical model limitations in Medlyn et al., 2016). van der Sleen et al. (2015) argues that historical increases in CO_2 (1850–2000) do not show significant fertilization effects on tropical tree growth, suggesting that some models are overestimating tropical CO_2-driven biomass accumulation, perhaps due to a lack of nutrient constraints or accurate mortality representation. Therefore, the scope of this study was to evaluate the direct "CO_2 effect" (β response) on the tropical forest sink as CO_2 increases and as represented across multiple model approaches. The β response represents the single largest source of uncertainty in terrestrial ecosystems projections of net ecosystem exchange of CO_2 (Cox et al., 2013; Friedlingstein et al., 2014; Sitch et al., 2015). Our intent is to highlight the major controls over tropical forest CO_2 response in vegetation that is dynamically structured vs. unstructured, in order to identify processes that should be priorities for future ESM development with regard to direct CO_2 effects and improving simulations of tropical forests.

2. Methods

2.1. Forest Inventory Data

Forest inventory data for use in model benchmarking were collected over two intersecting 5-ha transects (20 × 2,500 m) at the ZF2 Estação Experimental de Silvicultura Tropical (EEST) operated by Brazil's National Institute of Amazonian Research (Instituto Nacional de Pesquisas da Amazônia—INPA), located in the Cuieiras Reserve (2.45–2.66° S, 60.02–60.32° W), 53-km north of the city of Manaus, Brazil (Figure 2); see Negrón-Juárez et al. (2015) and supporting information, section 1 for more site-level information and field inventory synthesis. The site has had minimal human disturbance and is classified as an old-growth primary forest dominated by oxisol soils with local relief up to 50 m. The two transects (10 ha) are crossed by small streams in valleys (Figure 2a), with soils varying from high clay content to white sand soils (de Carvalho Conceição Telles et al., 2003), cover a range of plateaus to valleys, with high species diversity (856 species), similar to forest dynamics at the landscape scale.

The ZF2 transects were established in 1996, with field inventories conducted in 1996 and every two years from 2000 to 2010, and again in 2011 for a 15-year dataset, with a total of nine census intervals. In each inventory, the diameter at breast height (DBH, cm) was recorded for all trees larger than 10-cm diameter. Tree diameter was then converted to aboveground biomass (AGB) using allometric relationships obtained through destructive sampling of trees near the study site (Chambers, Santos, et al., 2001). Growth increment was estimated as the annual change in biomass for trees that were still alive, with biomass allometrically tied to changes in DBH. Loss from mortality was calculated by accumulating the biomass of trees that died in each interval, using biomass estimates from the previous survey, and annualizing the loss. In all cases, the mortality fluxes did not include a litter flux from live trees. We compared AGB (Mg ha^{-1}), growth increment (G; Mg ha^{-1} $year^{-1}$), mortality flux (M; Mg ha^{-1} $year^{-1}$), net increment (Δ) (where $\Delta = G - M +$ recruitment of new trees into the >10-cm size class) all reported as dry biomass, and growth fraction (%) from field observations for years 1996–2011 to model predictions.

2.2. Simulation Protocol

Simulations with ED2, ELM-FATES, CLM5, and ELMv1-ECA were conducted at the ZF2 old-growth lowland forest site, with the main differences between model processes, operations, and key parameters for each of the four models described in Table 1. Following common modeling protocols (Zhang et al., 2015), all models were updated to use the same soil texture parameters (i.e., soil fractions of 70% clay and 20% sand, based on field data) and site-level meteorological climate-forcing data, to eliminate model biases contributed by edaphic factors or climate forcings. Apart from these changes, no site-level tuning was conducted with the models. Aside from ELM-FATES, which is a new model that required some parameterization development, each model were each run "out of the box" to avoid site-specific over-tuning, thus allowing for model evaluation based on their default configurations and relatable to simulations across the broader central Amazon region (see section 2b in the supporting information for a description on ELM-FATES sensitivity tests).

All models were driven by climate-forcing data derived from measurements at the eddy covariance flux tower at kilometer 34 (K34) of the ZF2 road. The measurements included precipitation, downwelling shortwave radiation, downwelling thermal (longwave) radiation, air temperature, relative humidity, and wind speed. Processed data from 2000 to 2008 were used to drive the models using 30-min averages, which were cycled repeatedly throughout the simulations, another widely used site-scale modeling approach to simulate longer time periods (de Almeida Castanho et al., 2016; Zhang et al., 2007). Atmospheric pressure was held constant at 1,000 millibars. We opted to use tower-based climate drivers due to large biases in re-analysis meteorology and resulting biases in model predictions of land processes using re-analysis forcing (Niu et al., 2017; Zhang et al., 2007). Medvigy et al. (2010) highlighted the importance for climate driver data to include high intradiurnal variability, which is typical of site-level tower data. The ED2 model has shown strong sensitivity to large-scale meteorological precipitation inputs, that is, overestimates "drizzle" and leads, for example, to large overestimations of leaf evaporation due to inadequate canopy throughfall in ED2 (Knox et al., 2015). We also used recorded measurements of sensible heat, latent heat, and derived GPP from the K34 eddy covariance flux tower to evaluate modeled seasonal cycle for all models, which has been more fully investigated by (Restrepo-Coupe et al., 2013) at this site.

Figure 2. (a) False color IKONOS image (dry season 2001) of the field experiment site. Intersecting gray lines show the location of the two transects (5 ha each) compared to local topography and the ZF2 road, which the curving feature that touches the North and Eastern tips of the two transects. Leafless drought-deciduous trees are evident as red crowns. (b) A visible image showing the geographic position of the field site (marked as "ZF2-EEST") in context of the Amazon basin biome and geopolitical boundaries courtesy of Google Earth.

All model simulations employed a 350-year spin-up phase beginning at year 1500 until vegetative biomass became stable under preindustrial (1850) CO_2 concentrations (i.e., 292 ppm). A broadleaf evergreen tropical tree was the main plant functional type (PFT) for all model simulations here, although these models can be run with multiple tropical PFTs. The scope of this study was to evaluate the direct β effect on the tropical forest sink over time as CO_2 increased, maintaining climate drivers unchanged. The modeled trajectory of CO_2 concentrations was imposed using a simple third order quadratic approximation that fits the global historical mean and IPCC scenario IS92a projections (Chambers, Higuchi, et al., 2004; IPCC, 2000). The simulations were continued through an idealized historical and future projection phase, in which CO_2 concentration increased from preindustrial levels to a doubling of present-day CO_2 in 2073, after which eCO_2 was held constant at 584 ppm until 2100. To evaluate effects of constant doubled CO_2, we extended the simulations to 2200 at 584 ppm CO_2.

We used a quasi-factorial design to test vegetation demography and plant competition for nutrients separately as critical processes to tropical forest dynamics and CO_2 fertilization responses (Levine et al., 2016). For example, the two big-leaf models used here allow for evaluation of dynamic approaches that allows plants to adjust C assimilation in response to climate and atmospheric CO_2 change, and environmental stresses, including water, nutrient availability (N in CLM5, and N and P in ELMv1-ECA), and light. Currently the two VDMs do not include changes to allocation based on nutrient competition and essentially represent C-only processes. Through demography these VDMs will vary in size-structured forest composition, with different plant types competing for light within the same vertical profile, as well as heterogeneity in light availability along disturbance and recovery trajectories. To isolate the nutrient effects from demographic effects we ran the two big-leaf models in their C-only modes. This allowed for direct comparison of unstructured, aggregated vegetation to the VDM predictions using highly resolved demographic processes and the effects of each approach on current and long-term biomass predictions (Figure 1).

2.3. ED2 Simulation Specifications

The ED2 simulations were initialized with equal and low number densities of saplings from three forms of a broadleaf evergreen tropical PFT: early successional, midsuccessional, and late successional PFTs at the ZF2 site. These variants differ in four functional traits (wood specific gravity, maximum photosynthetic capacity, leaf lifespan, and specific leaf area), which further serve as a basis for prediction of a number of other

functional traits (Moorcroft et al., 2001). See Knox (2012) and Longo et al. (2019) for specific references on model equations and assumptions. The ED2 photosynthesis solver is based on the model of Farquhar, von Caemmerer, and Berry (FvCB) (Farquhar et al., 1980), using the temperature-dependent functions of photosynthesis (within the Rubisco-limited CO_2 demand) from Collatz et al. (1991) (Q10 equation). ED2 estimates rates of tree mortality that vary as a function of plant size and functional type. See supporting information; section 2a (Table S1), for more information on the three mortality terms that encompass five mortality processes.

The ED2 simulation started in the year 1500 to allow the vegetation competitive growth, mortality, and recruitment dynamics to reach biomass equilibrium. Equilibrium in this context is determined if the stand total biomass of each plant functional type remained stable over interdecadal time scales under the tower data's hydrologic climate forcing loop and preindustrial carbon dioxide concentrations. Within 250 years the biomass of the late successional broadleaf evergreens stabilized as the dominant functional type and the early successional broadleaf evergreens stabilized as the subdominant functional type in terms of biomass.

2.4. ELM-FATES Simulation Specifications

ELM-FATES is an age and size-structured VDM coupled with the E3SM Land Model (ELM) v1, a critical addition for representing disturbance-partitioned landscapes in ESMs (for documentation, see https://fates-docs.readthedocs.io/en/latest/index.html). The underlying concepts and vegetation dynamics in ELM-FATES are based on the ED model (Moorcroft et al., 2001), including individuals represented as cohorts (i.e., similar plant type and height), patch "time-since-disturbance" concept, and plant trait filtering. A major and first development was coupling the ED concepts to the physical processes inherit to the CLM land surface scheme, as described in R. A. Fisher, McDowell, et al. (2010) and Fisher et al. (2015) for the development of CLM (ED). The demographic and disturbance components were then detached from CLM (ED) to create FATES along with significant development including updates to canopy physics, allocation and allometry, the approach for canopy competition and sorting, and the representation of disturbance.

For example, a major modification is the adoption of the perfect plasticity approximation (PPA) (Purves et al., 2008) used for the accounting of canopy crown spatial arrangements by scaling from individual plants to a multilayered forest canopy based on available light and cohort height, a more detailed description in Fisher et al. (2018). Further updates include multilayer multi-PFT radiation transfer, a target C allocation to storage, and a proxy for hydraulic failure tree mortality related to soil moisture potential. ELM-FATES calls for four allometric models (tree height, crown area, sapwood cross-sectional area, and target biomass for six separate pools), allowing for dynamic competition and varying size structure. As with ED2, the additional forms of plant mortality in these ELM-FATES simulations are based on C starvation, tree-fall impact mortality, and a background mortality rate (0.009 N $year^{-1}$). Following CLM5, ELM-FATES photosynthesis is also based on FvCB (Farquhar et al., 1980), but unlike ED2, it uses the original Arrhenius equation from Farquhar et al. (1980) and also accounts for the maximum potential rate of electron transport (J_{max}) within the light-limited photosynthesis rate calculation, as well as the triose-phosphate utilization limitation. Other photosynthetic mechanisms are derived from CLM4.5 (Oleson et al., 2013).

Calibration of ELM-FATES is at a less mature phase than the other models used herein. Through sensitivity tests of ELM-FATES conducted here, we determined that several tropical parameters needed to be adjusted to generate more realistic tropical forest attributes and size structure distributions (Figure S1): target C storage as a ratio of leaf biomass ($S_{cushion}$), parameters controlling allometric crown area spreading (m^2 cm^{-1}) of each canopy layer (S_c), the canopy threshold fraction at which light competition begins to impact tree growth (A_t), specific leaf area (SLA), and senescence mortality rates. See supporting information, section 2b for a more detailed description of the sensitivity analysis of ELM-FATES for robust simulations of demographically structured forest dynamics. An advantage of including ELM-FATES in this study is the linkage between a VDM with the surface energy fluxes and physiology concepts in ELMv1 (see Figure 3 for closest match of fluxes between ELM-FATES and observations). The ELM-FATES simulations included a single broadleaf evergreen tropical tree PFT, and during the 350-year spin-up period, vegetation successfully reached equilibrium prior to the post-industrial CO_2 concentrations changes at 1850.

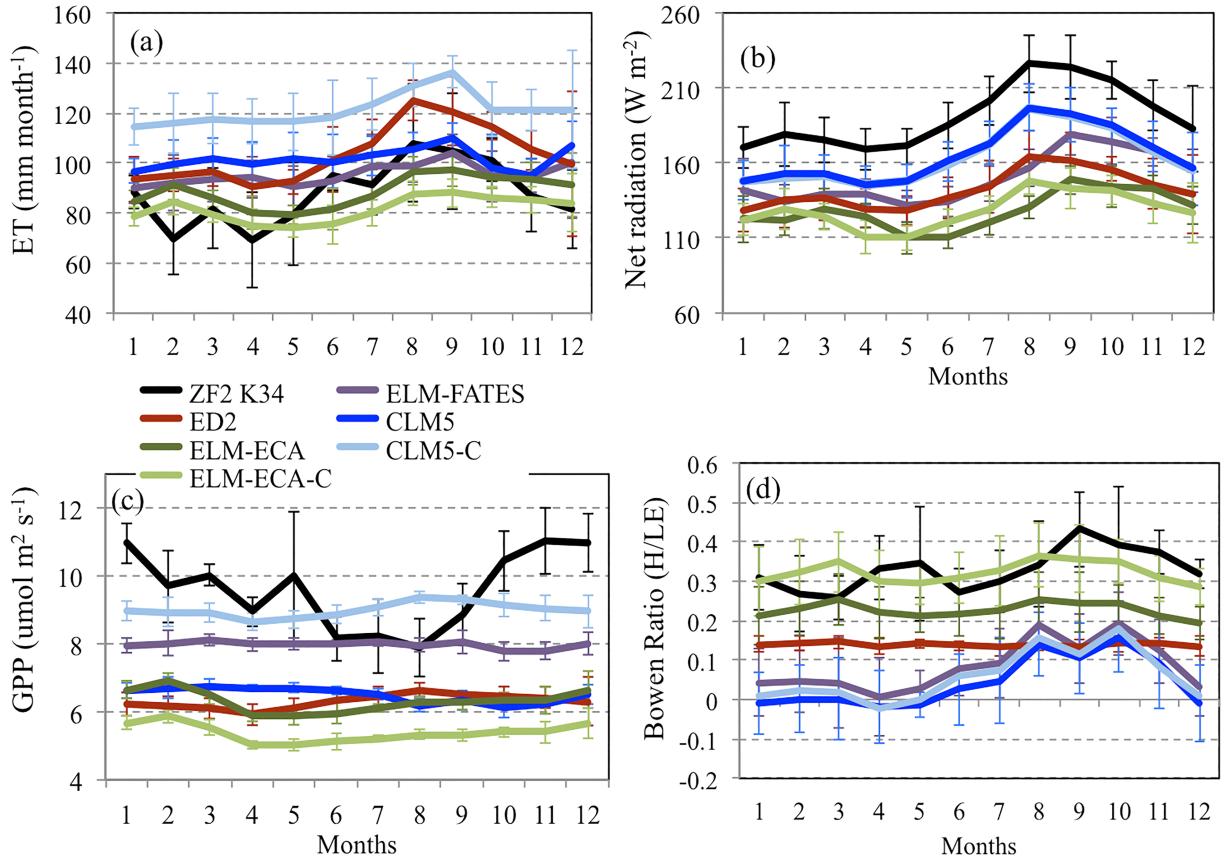

Figure 3. Observed vs. modeled (a) evapotranspiration (ET) defined as sum of soil and vegetation evaporation and transpiration; all models except for ELMv1-ECA-C overestimated ET (annual average higher by +0.5 to +33 mm month^{-1}). (b) Net radiation (R_n; W m^{-2}); all models underestimated R_n (annual average lower by −26 to −63 W m^{-2}). (c) Gross primary productivity (μmol m^2 s^{-1}) (GPP), and similar to R_n all models underestimated GPP (annual average lower by −0.6 to −4.2 μmol m^2 s^{-1}). (d) Bowen ratio defined as sensible heat (SH) divided by latent heat (LH). Panels (a)–(d) use observed data from K34 tower at ZF2 averaged from 2000 to 2008, and model results averaged over 2000–2010.

2.5. CLM5 Simulation Specifications

CLM5 (Lawrence et al., 2019; Oleson et al., 2013) is the land model for the Community Earth System Model version 2 (CESM2.0) and is a terrestrial model with prognostic biogeophysics and biogeochemistry (BGC). CLM5 operates as a "big-leaf" land surface model that represents the plant canopy in an aggregated manner and has constant mortality and stem turnover (Table 1). Substantial updates have been made to the plant nutrient dynamics in an effort to reduce structural uncertainty in the CLM4.5 representation of N limitations and downregulation (Ghimire et al., 2016; Keller et al., 2017; Zaehle et al., 2014). For example, N uptake imposes a C energy cost, symbiotic N fixation is represented (Brzostek et al., 2014; J. B. Fisher, Sitch, et al., 2010; Shi et al., 2013), and plant C:N ratios are now variable (Ghimire et al., 2016). This approach replaces the "relative demand" (RD) approach of downregulating potential GPP (i.e., limiting net photosynthetic rate) based on the relative demand of plants and soil microbes.

Allocation of C is not dynamic in CLM5 and always allocations the same fixed fraction to plant tissues. A new plant hydraulic stress routine has been included, where vegetation water potential is forced by transpiration demand and soil water potentials (Kennedy et al., 2019). The former stomatal conductance from CLM4.5 (Ball et al., 1987) has been updated to the conductance model of Medlyn et al. (2011) due to its more realistic behavior at low humidity levels. It is known that, at a global scale, CLM5 has a higher response to CO_2 fertilization than other versions of the CLM which included the relative demand approach (Wieder et al., 2019).

We initialized CLM5 from a 1,000-year "accelerated decomposition spin-up" simulation (Koven et al., 2013), followed by a standard equilibration run starting at year 1500. Simulations were run within a 1° grid cell (100

km^2) that covered the ZF2 field site and was used to define the surface properties. We used a mass balance approach between annual changes in AGB and losses due to mortality (M) to calculate the plant growth flux (G) in CLM5. We calculated N use efficiency (NUE) as NPP divided by plant N uptake. The CLM5 C-only simulations were achieved by activating the mode to supply unlimited N in the BGC submodel, which was simulated over the 350-year spin-up and into the historical and future time periods (1850 to 2100), thus eliminating plant growth limitations due to N competition. The N addition averaged ~0.21 gN m^{-2} $month^{-1}$ over the present-day period, which lead to a 11% increase in soil N.

2.6. ELMv1-ECA Simulation Specifications

We also used a "big-leaf" version of ELM (ELMv1-ECA; Zhu & Riley, 2015; Zhu et al., 2016, 2017; Riley et al., 2018), which incorporates coupled C, N, and P dynamics. The original version of ELM is based on CLM4.5. Major updates in ELMv1-ECA include (1) consideration of the P cycle (Wang et al., 2007), (2) inclusion of ECA kinetics theory for trait-based plant-microbe nutrients competition (replacing the RD concept; Tang & Riley, 2013), (3) flexible and prognostic vegetation C:N:P stoichiometry and its effects on plant photosynthesis (Ghimire et al., 2016; Walker et al., 2014), and (4) dynamic C allocation following the structure of Friedlingstein et al. (1999). This model directly links fine root biomass to the nutrient competitiveness of roots, consequently, the amount of nutrient taken up by plant. Therefore, dynamic allocation is directly linked to nutrient dynamics.

The simulation protocol for ELMv1-ECA is similar to CLM5, with the only difference being that after the "accelerated decomposition spin-up phase," soil inorganic phosphorus pools (labile P, solution P, secondary P, occluded P, and parent material P) are initialized with Hadley P fractionation observations at tropical lowland forest ecosystems (Yang et al., 2013). The model continued for another 350 years in "regular spin-up" mode with C, N, and P fully prognostic, with transient simulation from 1850 to 2200. As with CLM5, simulations were run using a 1° grid cell (100 km^2) that was used to define the surface properties, which covered the ZF2 field site with 100% broadleaf evergreen tropical tree cover. ELMv1-ECA simulations include annual N and P deposition based on Lamarque et al. (2010) and Wang et al. (2015), respectively. Losses due to mortality, plant growth flux, and annual changes in AGB were calculated as in CLM5. We calculated P use efficiency (PUE) as NPP divided by plant P uptake.

The ELMv1-ECA C-only simulations were achieved by activating the modes to supply both unlimited N and P in the ECA submodel, which was simulated over the 350 year spin-up and into the historical and future time periods (1850 to 2100), thus eliminating plant growth limitations due to NP competition. The N addition and P addition averaged ~0.008 gN m^{-2} $month^{-1}$ and ~0.004 gP m^{-2} $month^{-1}$ over the present-day period, which lead to a 42% and 11% increase in soil N and soil P, respectively.

3. Results

3.1. Evaluation of Present-Day Forest Demographics and Energy and Water Fluxes

At the ZF2 transects, which capture landscape-scale forest variability, observed forest biomass balance was nearly neutral for 15 years, with a mean annual net increment of 0.09 ± 1.95 Mg ha^{-1} $year^{-1}$ in AGB (0.03% of its mean mass) (Table 2). Observed annual growth and mortality fluxes were roughly balanced and the small positive net increment was due to the incoming recruitment flux (see supporting information, section 1). ED2 agreed best with AGB field estimates (within approximately +3% mean AGB), while the two ELM models underestimated AGB (ELMv1-ECA: −69% difference; bias = −156 Mg ha^{-1} and ELM-FATES: −22% difference; bias of −60 Mg ha^{-1}), and CLM5 slightly overestimated AGB (+16% difference; bias = +52 Mg ha^{-1}). However, ED2 overestimated growth and mortality fluxes, and the overestimation of growth (almost double the field data) compared to the mortality flux resulted in large positive annual net increments over time (1.2 ± 0.47) (Table 2). The growth and mortality fluxes predictions from ELM-FATES, ELMv1-ECA, and CLM5 were within ~18% (growth) and ~35% (mortality) of field measurements despite less accurate estimates of total biomass. None of the models matched the neutral net biomass increments observed in the census, although ELMv1-ECA was the closest: 0.43 ± 0.46 Mg ha^{-1} $year^{-1}$.

As a prerequisite for overall carbon predictions, we further evaluated model predictions of seasonal energy, carbon, and water fluxes (evapotranspiration (ET), net radiation (R_n), GPP, Bowen ratio (sensible (H) divided by latent heat (LE) fluxes), and annual LH) at the well-studied central Amazon site (Araújo et al.,

Table 2
Mean Aboveground Biomass (AGB) ± Standard Deviation, Fluxes of Living Trees, Annual Net Increment, Linear Coefficient Trends (all in Mg ha^{-1} year^{-1}) Using Least Square Regression Along With the Standard Error in Parentheses, and Total AGB Accumulation Over the 15-Year Period as Measured at the ZF2 Field Site From 1996 to 2011, and Estimated by the Four Models, as Well as the Carbon-Only Versions of the Two Biogeochemical Models (CLM5-C and ELMv1-ECA-C)

	ZF2 Field	ED2	ELM-FATES	CLM5	CLM5-C	ELMv1-ECA	ELMv1-ECA-C
Mean AGB (Mg ha^{-1})	303 ± 2.3	311 ± 4.2	243 ± 4.8	355 ± 3.6	506 ± 6.3	147 ± 4.1	245 ± 4.0
Growth increment (G) (Mg ha^{-1} year^{-1})	4.52 ± 1.22	8.03 ± 0.49	4.72 ± 0.35	5.45 ± 0.28	8.05 ± 0.36	4.03 ± 0.23	9.54 ± 0.34
Mortality (M) (Mg ha^{-1} year^{-1})	5.01 ± 1.68	6.83 ± 0.98	3.53 ± 0.23	4.54 ± 0.04	6.48 ± 0.07	3.59 ± 0.05	8.70 ± 0.12
Annual net increment (Δ) (Mg ha^{-1} year^{-1})	0.09 ± 1.95	1.20 ± 0.47	1.19 ± 0.23	0.91 ± 0.26	1.57 ± 0.32	0.43 ± 0.46	2.30 ± 0.34
Linear coefficient trend (Mg ha^{-1} year^{-1})	0.003 (0.12)	1.2 (0.05)	1.2 (0.03)	0.9 (0.06)	1.5 (0.07)	0.4 (0.05)	0.8 (0.07)
15-year AGB accumulation (Mg ha^{-1})	−1.38 ± 4.49[b]	17.97	17.24	13.3	23.4	6.66	12.5
Long-term AGB sink[d] (Mg ha^{-1} year^{-1})	0.46[a] to 0.9[c]	1.04	0.80	0.77	1.24	0.10	0.66
Long-term relative Δ AGB (%)	N/A	78.3	87.4	48.0	56.0	21.0	63.8
AGB amplitude (Mg ha^{-1})	6.6	3.4	2.9	2.3	4.5	1.7	2.8

Note. Mortality (M) is the average annual aboveground mortality flux due to death of an individual (this does not include maintenance litter fluxes of living trees). Growth increment (G) is the average annual accumulation of AGB in live trees. The net increment as calculated by the models is (Δ) = G − M, due to inability to calculate a recruitment flux in the big-leaf models. The field dataset has a diameter threshold of 10 cm, and new trees entering this threshold were accounted for, therefore a recruitment flux (R) for the mass of newly recruited plants was used (i.e., 0.58 Mg ha^{-1} year^{-1}) to close the observed mass balance, where Δ = G − M + R. The error terms for (Δ) were calculated using the annual 1996–2011 values for (Δ) = G − M. Model response compared to site-level field observations for the long-term biomass sink and interannual amplitudes in AGB over each cycle from 1900 to 2000.
[a]Baker et al. (2004) after separating the Brazilian forests from the Amazon basin. [b]Standard deviation of AGB accumulation between the two ZF2 transects (5 ha each). [c]Aragão et al. (2014); Brazilian Amazon. [d]Field data: maximum of 22 years (Baker et al., 2004); 24 years (Aragão et al., 2014); Models: over 200 year period 1900–2100.

2002). While a large spread emerged, the models best predicted monthly ET, a key water variable for linkages to ecosystem functioning and carbon feedbacks (Fisher et al., 2017), with ELMv1-ECA and ELM-FATES models most similar to observations (Figure 3a). With respect to ED2, Wehr et al. (2017) reported that ED2 captured overall ET for a temperate forest, but with unrealistic partitioning between transpiration and ground evaporation indicating model predictions remain uncertain. The remaining three fluxes were all underestimated by all four models. Each model underestimated R_n, but successfully captured its seasonal cycle (Figure 3b). Each model also underestimated average monthly GPP, with little variation across seasonal cycles, compared to a substantial dry season decline in the observations (Figure 3c). Following the same trend, all models predicted a lower Bowen ratio except for ELMv1-ECA-C (Figure 3d), primarily due to lower modeled H compared to observations, 27.6 W m^{-2}. The more productive C-only version of ELMv1-ECA predicted both H and LE similar to observations. For each of the energy, carbon, and water fluxes the largest range was between the two big-leaf models.

An interesting outcome was ELMv1-ECA-C reported lower GPP and ET than ELMv1-ECA, even though the C-only simulation produced larger stand biomass (Table 2). This was a result of differing V_{cmax} schemes (i.e., a critical parameter defining the maximum rates that enzymes drive photosynthesis) and leaf N and P concentrations. The C-only version used fixed values of V_{cmax} and leaf C:N. Alternatively ELMv1-ECA predicts V_{cmax} as a function of leaf N and leaf P relationships. These different schemes result in C-only simulations having lower prescribed V_{cmax} (lower photosynthesis and GPP) and lower prescribed leaf N (lower AR), therefore, higher net product (NPP = GPP − AR) and biomass (Figure S2a). An additional explanation is with no limitation of nutrients in ELMv1-ECA-C, there was no need for a shift in C allocation to fine root production (seen in Figure 7b), thus lower leaf N in ELMv1-ECA-C (8.5 gN m^{-2}) compared to ELMv1-ECA (9.8 gN m^{-2}) (Figure S2b) contributing to the larger difference in AR in ELMv1-ECA-C. With regards to lower ET in ELMv1-ECA-C, ET and GPP are tightly linked in ELMv1 due to calculating stomatal resistance based on the Ball-Berry conductance model, which influences ET and tracks GPP.

3.1.1. Demographic Model Output and Field Inventory Size-Structured Data

By comparing against the detailed 15-year forest inventory dataset we were able to provide insight into how the VDMs predicted vegetation size structure and how ELM-FATES compared to ED2 (Figure 4). The census observations showed patterns typical of an old-growth tropical forest: reduction in basal area with increasing tree size (Figure 4a), small diameter increments that increase with size (Figure 4b), steep reductions in stem density with size (Figure 4c), a large number of trees that showed no growth across size classes (Figure 4d), and low mortality rates for stems >10 cm DBH that increased slightly with size (Figure 4e). Both VDMs

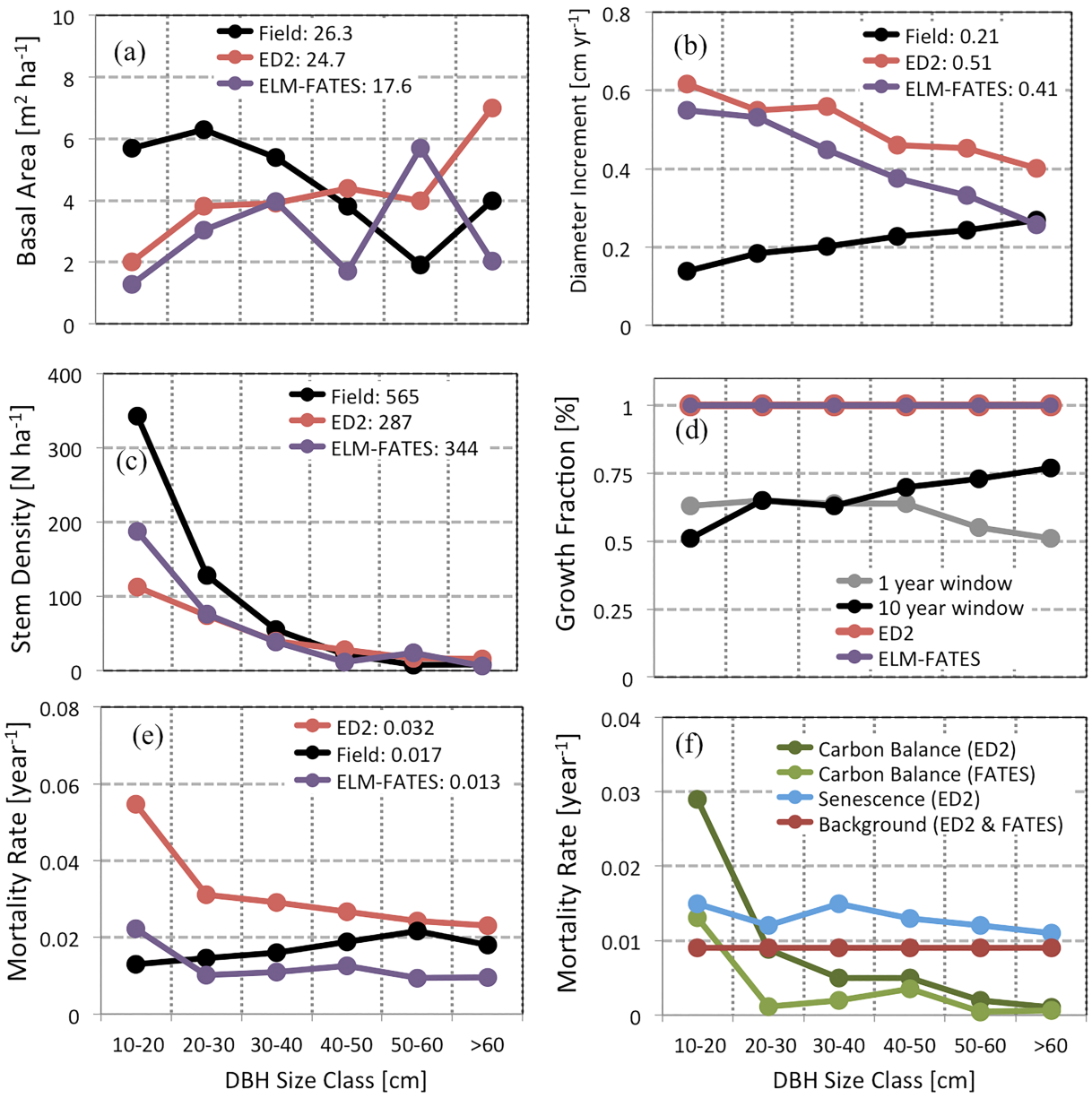

Figure 4. Field data (black circles) and ED2 and ELM-FATES model estimates of (a) basal area, (b) mean diameter annual increment, (c) stem abundance, (d) fraction of trees showing detectable growth (>1-mm increment in diameter) reported by the two models and averaged over time windows of 1 and 10 years of inventory measurements, (e) mean annual mortality rates across size classes, (f) mean mortality rate partitioned by mechanism, separated by DBH (cm) size classes and both field data and models predictions averaged from 1996 to 2011 corresponding to the full 15-year inventory. Values in figure legends correspond to the mean value over all diameter classes.

predicted lower basal areas in all trees <40 cm and greater basal area in all trees >50 cm, in contrast with field observations, with one exception being the largest size class (>60 cm) in ELM-FATES. Biomass increment plots (Figure S3) showed that half of forest biomass in the transects is contained in the top 11% largest trees and half of the growth increment is contained in the top 20% largest trees (confirming Figure 4b). However, the two size-structured models showed the opposite pattern (decreasing growth with size class) and overestimated mean diameter increment, particularly in smaller sized stems (Figure 4b). Overestimates of growth rates in both models could be due to low stem density (Figure 4c), and subsequent reduced light competition, among other factors. ELM-FATES had stem density predictions closer to the observations compared to ED2, particularly in the smallest size class.

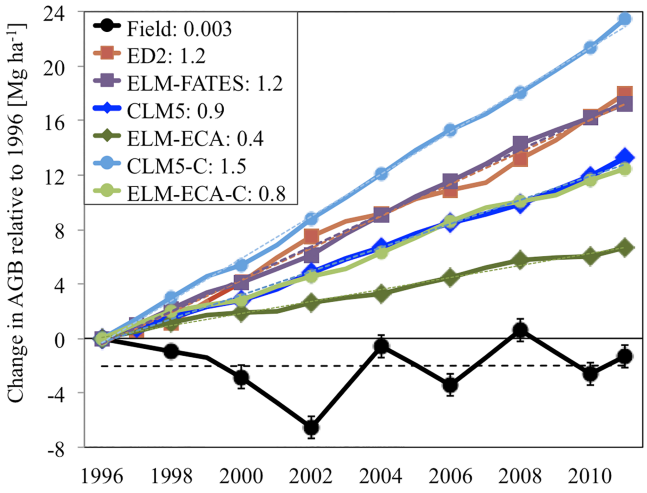

Figure 5. Annual mean aboveground biomass relative to the 1996 estimate (ΔAGB) as measured in the field (black line), and estimated by two VDMs (squares), two aggregated vegetation biogeochemical models (diamonds), and the same two aggregated vegetation models, but their carbon-only variants (circles). Least squares regression is used to calculate mean trends and coefficients over the 1996–2011 interval and can be found in Table 2.

In both VDMs, virtually all trees across all size classes exhibited positive diameter growth increments and thus accumulated woody stem biomass, in contrast to the observations (Figure 4d). In the field data as many as 50% of trees in the lowest size class showed no detectable growth, even when observed over the entire 15-year inventory period. In larger size classes (>60 cm) trees that had no growth ranged from 25% to 50% of stems depending on the length of the observation window chosen (i.e., 10- or 1-year windows, respectively). We found that ED2 compensated for high growth with correspondingly high mortality rates (overestimated by 85%, 0.032 vs. 0.017 year^{-1}) and weak rate of ingrowth into the 10 cm DBH class leading to lower total stem density compared with census data (287 vs. 565 N ha^{-1}) (Figure 4e). These high mortality rates in ED2 were dominated by the density-dependent C starvation mechanism (Figure 4f). We ruled out overestimation of understory light competition, after ED2 estimates of vertical radiation scattering were accurately benchmarked against published data of height structured light competition (Cabral et al., 1996; Mercado et al., 2007), (Figure S4 and supporting information, section 3b). The overestimation of C starvation was likely due to uncertainty in the relationship between carbon balance ratio (CBR, i.e., an appraisal of the plant's actual carbon acquisition versus its potential carbon acquisition under optimal conditions) and the mortality rates determined from these ratios. ELM-FATES estimated total mortality rate closer to observations (0.013 vs. 0.017 year^{-1}), mainly via a lower C starvation mortality (Figure 4f).

3.1.2. Evaluation of Current Biomass Trends

Typical of quasi-equilibrium mosaic landscapes, AGB at ZF2 (Figure 5, Table 2) showed pronounced interannual variability (mean of 3.40 Mg ha^{-1}), with a neutral mean annual C sink (0.003 Mg ha^{-1} year^{-1}) when using a linear fit. Summed over the 15-year study period, AGB accumulation was negative (−1.38 Mg ha^{-1} year^{-1}). Though mean annual net increments from all models were within the error estimate of the inventory data (1.95; Table 2, Row 4), all models showed close to no interannual variability and predicted constant positive ΔAGB trends (1.2, 1.2, 0.9, and 0.4 Mg ha^{-1} year^{-1} for models ED2, ELM-FATES, CLM5, and ELMv1-ECA, respectively). This led to large modeled 15-year total biomass accumulations (17.97, 17.24, 13.30, and 6.66, respectively, for models vs. −1.38 Mg ha^{-1}, Table 2). The 15-year total biomass accumulation was lowest for ELMv1-ECA because of its strong P-cycling restrictions on GPP, as discussed below.

We compared the landscape-representative ZF2 transects and all model results against average annual net biomass accumulation rates across other Brazilian sites (Baker et al., 2004). A third of the sites had negative biomass change (no significant sink), confirming that ZF2 is not an outlier and that biomass neutrality is present across the region, but not consistently (Figure S5). The Brazilian field sites had an average sink of 0.46 Mg ha^{-1} year^{-1} with a large standard deviation of 1.49 Mg ha^{-1} year^{-1}. Therefore, all predictions of net annual biomass accumulation from the models (which were not site tuned and remained in their original, generic regional calibrations) fell within this standard deviation range. Within the VDMs used here, stochastic mortality events are smoothed out by grouping trees into representative classes and averaging across multiple disturbance patches (<1-ha scale), thus muting any large local variability in biomass flux due to episodic, large mortality events. However, interannual variability was captured when evaluating mortality rate in terms of number of stems (stems year^{-1}) (Figure S6) and is a better comparison and good local-scale benchmark.

3.2. Modeled Long-Term CO_2 Sensitivity and Biomass Projections

Under an idealized long-term CO_2 fertilization scenario in which CO_2 concentrations grow exponentially until they were capped at doubled preindustrial values in 2073, three of the four models estimate that the central Amazon forest remains a large long-term biomass sink from 1900 to 2100 (Figure 6), increasing concurrently with CO_2. Differences in magnitudes of the biomass sink, timing response relative to the CO_2 signal, and decadal fluctuations emerge due to each model's conceptual and mechanistic differences. Over 200 years (1900–2100), the spread in predicted total forest biomass sinks was very large (Figure 6a; 179 Mg ha^{-1}).

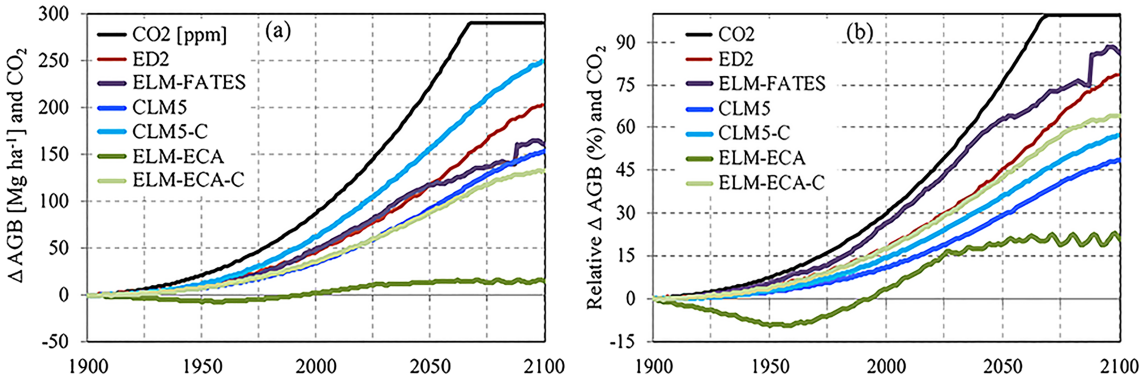

Figure 6. Projected biomass estimates to 2100 (right y-axis) relative to preindustrial values (year 1900), at the central Amazon ZF2 site from four terrestrial biosphere models, with two baseline simulations of the big-leaf models as unconstrained carbon-only model versions (CLM5-C and ELMv1-ECA-C). ΔAGB reported as (a) absolute change in AGB (Mg ha^{-1}) from 1900 values, with modeled annual biomass increment (Mg ha^{-1} year^{-1}) increasing by (from lowest to highest) 0.10, 0.66, 0.77, 0.80, 1.04, and 1.24 Mg ha^{-1} year^{-1} for ELMv1-ECA, ELMv1-ECA-C CLM5, ELM-FATES, ED2, and CLM5-C, and (b) relative change in AGB (%) from 1900 values. Left y-axis on both panels (referencing the black line): Atmospheric CO_2 concentration driving the model simulations.

Assuming a linear trend the biomass sink for the models were 1.04, 0.80, 0.77, and 0.10 Mg ha^{-1} year^{-1} for ED2, ELM-FATES, CLM5, and ELMv1-ECA, respectively (Table 2). When evaluating *relative* ΔAGB (Figure 6b), by 2100 the increases in biomass were large for ED2, ELM-FATES, CLM5 (78%, 87%, and 48%, respectively) but only 21% change for ELMv1-ECA. Out of the two VDMs, ELM-FATES predicted lower current total AGB for this region (Table 2) contributing to a lower *absolute* biomass sink (Figure 6a) but enabling a higher potential for increasing biomass (Figure 6b). When nutrients are not constraining photosynthesis, CLM5-C predicted the largest biomass sink (1.24 Mg ha^{-1} year^{-1}), greater than the VDMs. ELMv1-ECA-C's predicted biomass sink increased from 0.10 to 0.66 Mg ha^{-1} year^{-1}, comparable to the nutrient-enabled version of CLM5, but slightly lower than the VDMs. The relative change in AGB by ELMv1-ECA-C (64%) was closest to estimates by the VDMs.

Averaged over the 2000–2010 period, the two big-leaf models have the highest C allocation to aboveground wood (~40%) compared to the other models and field data (34%), at the expense of C allocation to coarse roots (1%) vs. 8% in the field data (Figure 7a). The ZF2 site has very weathered nutrient poor soils compared to Amazonia (Baillie, 1996; Quesada et al., 2010), and as a result, tropical forests have high root production rates and faster turnover than other forested ecosystems (Silver & Miya, 2001; Vogt et al., 1995), making fine root growth C expensive. ELMv1-ECA was the only model that shifted C allocation to fine roots (for more P acquisition and compensating for faster turnover) in the 21st century (Figure 7b), contributing to the lower AGB response in ELMv1-ECA (Figure 6). With regards to the VDMs, the largest shift in C allocation was a *decrease* in fine roots allowing for more C accumulation in woody components, which should dampen once nutrient competition is introduced. Over the 21st century, higher N demand from eCO_2 was met with higher NUE, especially for CLM5 and ELMv1-ECA, increasing by 80% and 10%, respectively, compared to the 20th century (Figure 7b insert). The increase in PUE (89%) over the 21st century by ELMv1-ECA contributed to a stable biomass sink even under limiting conditions, with PUE increases due to changes in plant stoichiometry and shift towards more fine root allocation, allowing the plant to increase AGB.

Once CO_2 was capped (584 ppm) at year 2073, ED2 and CLM5 displayed inertia by continuing to increase in biomass for several decades (supporting information, section 4). We ran model simulations for another 100 years, to year 2200, to investigate AGB turnover rates (i.e., loss of tissues, Mg ha^{-1} year^{-1}), thus estimating longevity of biomass stocks under constant, doubled CO_2 compared preindustrial CO_2 (more information on modeled turnover rate in the supporting information, section 2c). All models showed an increase in vegetation turnover, thus shortening the longevity of C pools, except for ED2 which had a decreased turnover (Figure S7), contributing to a stronger biomass accumulation.

3.3. Model Differences Contributing to Divergent Biomass Projections

The contrasting predictions of modeled long-term woody NPP response between the VDMs and nutrient-enabled big-leaf vegetation models (Figure 8a) were an important contributor to the model

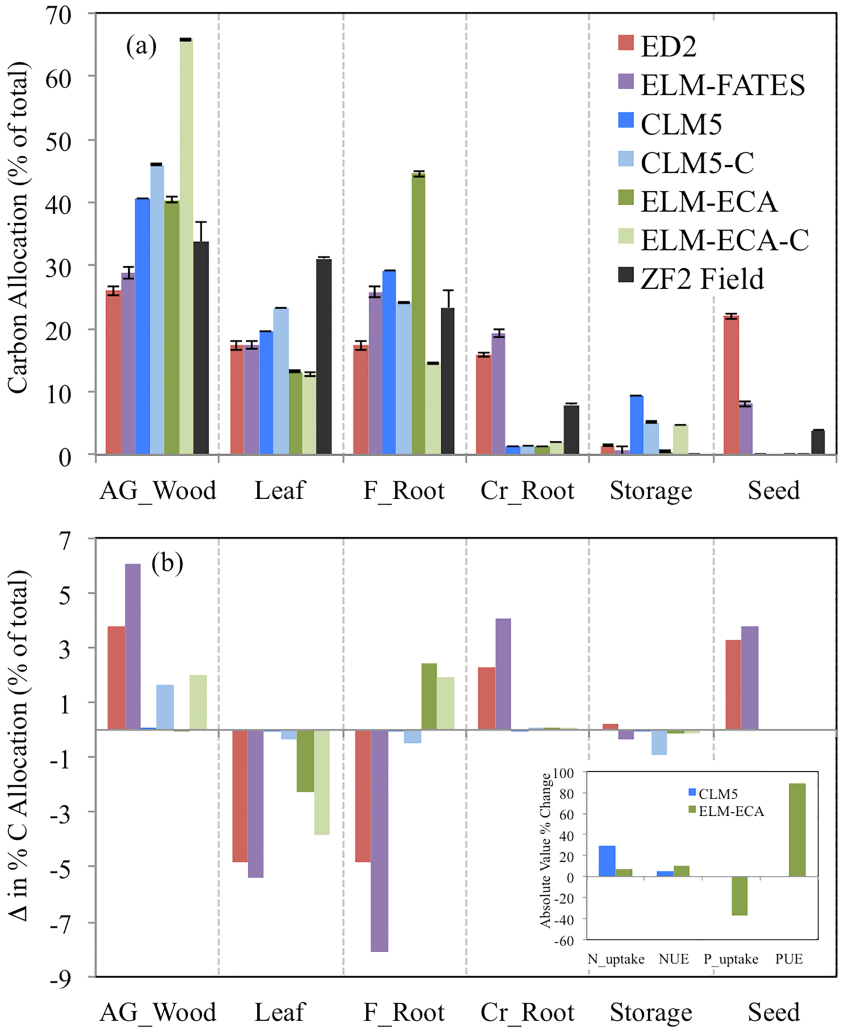

Figure 7. (a) Average carbon allocation (% of total biomass allocation) between the four models and the unconstrained carbon-only versions of the big-leaf models (CLM5-C and ELMv1-ECA-C) averaged from 2000 to 2010 (corresponding to the field data timeframe), ZF2 field data, across six plant production components (AG_wood = aboveground wood, F_Root = fine root, Cr_Root = coarse root). Field data estimates at ZF2 and K34 averaged from Chambers, Higuchi, et al. (2004), Chambers, Tribuzy, et al. (2004) and Malhi et al. (2009), data not available for storage. (b) Difference in the percentage of carbon allocation (% of total biomass allocation) between the 20th century mean (1900–2000) and 21st century mean (2000–2100) periods for each tissue component, across the four models. Insert: percent change (%) between the 20th century (1900–2000) and 21st century (2000–2100) periods for plant uptake of N, nitrogen use efficiency (NUE = NPP/N_uptake), plant uptake of P, and phosphorus use efficiency (PUE = NPP/P_uptake). CLM5 only includes N cycling.

divergence in biomass projections with eCO_2. Over 200 years with a doubling of CO_2, the two (C-only) VDMs predicted the largest increase in woody NPP (174% change, +10.6 MgC·ha^{-1}·year^{-1} for ED2 and 112% change, +6.9 MgC·ha^{-1}·year^{-1} for ELM-FATES) that was proportionally much greater than the increase in leaf area (9.8%, +0.4 m^2 m^{-2} for ED2 and 15.8%, +0.7 m^2 m^{-2} for ELM-FATES). This higher allocation to woody NPP was the primary driver of the simulated biomass response and likely influenced 100% of modeled trees experiencing positive growth (Figure 4d). In C-only mode, ELMv1-ECA-C also predicted a large response of NPP to eCO_2 (+70%) consistent with its excess biomass accumulation in the present-day simulation and larger than the version with nutrient limitations (+23%). CLM5-C also predicted a large NPP response (+58%), but this ended up being a smaller increase compared to CLM5 with nutrient constraints (+64%), oddly. ELM-FATES response of NPP to eCO_2 was lower and closer to the big-leaf models, compared to ED2. Even though CLM5 predicted a weaker increase in woody NPP compared to the VDMs, it still projected a large increase in absolute biomass, very similar to the VDMs (Figure 6). This larger biomass response in CLM5 could be a result of higher vegetation C:N ratio (Tang et al., 2018),

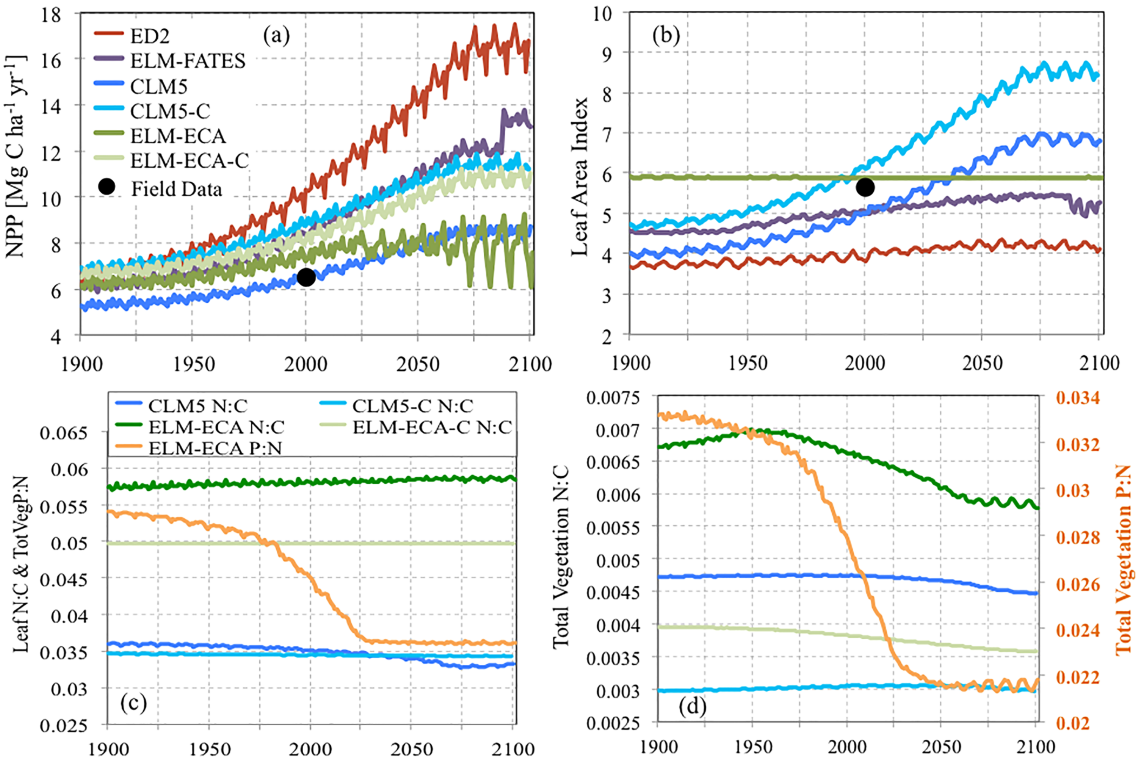

Figure 8. Model estimates from the four models and two baseline simulations of the big-leaf models as unconstrained carbon-only model versions (CLM5-C and ELMv1-ECA-C). Estimates for (a) mean annual NPP allocated to total woody biomass (above and belowground) and the ZF2 field measurement (black dot; 6.5 $MgC \cdot ha^{-1} \cdot year^{-1}$), (b) mean annual leaf area index (LAI) and the ZF2 field measurement (black dot; 5.7 $m^2\ m^{-2}$). (c) Mean annual leaf N:C for the big-leaf models and the C-only versions of these models, as well as leaf P:N for ELMv1-ECA. (d) Total vegetation N:C ratios for the nutrient-enabled models and their C-only versions and total vegetation P:N for ELMv1-ECA (right axis with different scales), indicating decreasing N and P quantity, two forms of nutrient limitation on GPP and NPP.

compared to the other big-leaf model (inverse of vegetation N:C; Figure 8d) or warrants further investigation. ED2 predicted the lowest LAI (~4 $m^2\ m^{-2}$), yet simulated the highest NPP and biomass sink, suggesting that assimilated and stored C was connected to processes other than phenology. Both ELMv1-ECA and ELMv1-ECA-C predicted the same LAI of 5.9 $m^2\ m^{-2}$ closest to observed values, although with no interannual variability or eCO_2 response. CLM5-C (which has constant leaf allocation fraction, and thus, no feedback control over leaf area) predicted the largest increase in leaf area index (LAI) (81% change; Figure 8b) and largest biomass accumulation out of the big-leaf models.

Evaluating changes to plant stoichiometry provides useful insight into potential photosynthetic C gain or acclimation with eCO_2. Both CLM5 and ELMv1-ECA showed a muted response of leaf N:C change to doubling CO_2 (Figure 8c), but a stronger decreasing trend of N:C ratio in total vegetation (Figure 8d). The nominal decrease in N:C ratios in CLM5 likely resulted from an increase in N uptake over the 21st century (Figure 7b insert). ELMv1-ECA produced a minor increase in leaf N:C with doubling CO_2 as a result of N-P interactions and shifts in fine root allocation that were only captured in the P-enabled model. ELMv1-ECA simulates a stronger decreasing trend in total vegetation N:C ratio (14% change) and leaf and total vegetation P:N ratio (Figures 8c and 8d, right y-axis) with eCO_2, indicating nutrient limitation on both GPP and NPP, resulting in a decreased biomass sink prediction. The interacting C-N-P cycles and C allocation schemes in ELMv1-ECA led to the lowest relative biomass sink (+21%) compared to the other models. The observed low soil P availability at ZF2 (Quesada et al., 2010), and the predicted importance of P under eCO_2, illustrates the importance of representing P feedbacks at this site.

By 2100, both VDMs predicted that individual trees progressed more quickly through size classes, shifting the biomass of the forest canopy structure towards larger size classes (Figures S8a and S8b), a diagnostic that is only available in the VDMs. For the case of ED2, this shift of the forest canopy towards larger trees

occurred mainly in the late successional PFT (Figure S8a). The increased leaf area of large trees and associated shading of the understory at the end of the 21st century drives higher carbon starvation mortality of understory stems, further contributing to a shift towards larger size classes. This enhanced mortality feedback which generates vigorous self-thinning (as seen by the highest modeled mortality in the smallest DBH size class in Figure 4f, but not in observations in Figure 4e) could provide insight into why the VDMs show higher NPP projections compared to the "big-leaf" models.

4. Discussion

The two VDMs (C-only ED2 and ELM-FATES) predicted this central Amazon site to act as a large forest biomass sink until 2100, likely an overestimate due to the lack of nutrient constraints in those models. This was confirmed by comparing the VDMs to the big-leaf models in either nutrient-enabled mode (lowest sink) or C-only mode, therefore no nutrient constraints and higher sinks similar to biomass sinks from the VDMs, confirming our main hypothesis.

CLM5 (N constraints only) also predicted a large biomass sink, even though photosynthesis became limited over time. ELMv1-ECA (with both N and P constraints) produced the most limited response to eCO_2 mediated by large P limitations on production, also confirming our main hypothesis.

Further addressing our hypotheses, the VDMs accurately captured trends in present-day demography and total biomass (Figure 4, Table 2). Improvements could be made with representing density-dependent (i.e., competition-induced) mortality processes, interannual variability in biomass, and lowering the continual increasing biomass accumulation (due to high woody NPP and growth), as well as incorporating constraints due to nutrients and more diverse life-history strategies. When considering present-day mean annual net increments (Δ), all models were within the large error estimates of the field data, but divergence from the neutral field data occurs in all models when considering the total 15-year biomass accumulation, with all the models showing a fertilization effect on biomass that is not evident in the data from this site.

These VDMs were designed to operate at the ESM scale but have never been fully tested for this application. While the demographic processes are slightly different between the two VDMs, this study takes a first step at showing the potential advantages of coupling FATES to an ESM's land surface model by comparing ED2 with ELM-FATES, which displayed a more realistically constrained absolute biomass sink, NPP flux, mortality rates, and LAI. We conclude that VDMs are applicable and fruitful at ESM scale (e.g., similarities or improved performance compared to unconstrained C-only big-leaf models), but more testing needs to be done over regional scales.

4.1. Goal 1: Uncertainties in Model Predictions Compared to 15-Years of Field Observations

4.1.1. Patterns and Uncertainties Related to Mortality

In the two VDM simulations, there was an underestimate of total stem density, likely due to an overactive density-dependent mortality and self-thinning of small trees, hence an overestimate of basal area of large trees (Figure 4a) contributing to the large biomass sink. Alternatively, stress-related mortality of very large tree could be underestimated. This highlights that predicting stem density can have strong dependence on model parameters. We suggest modeled density-dependent mortality (i.e., not background mortality) could benefit from more field-based mortality attribution (McDowell et al., 2018). For example, when mortality has been observed to be higher for the largest trees, these trends were dependent on life-form class (King et al., 2006; Manokaran & Kochummen, 1987), a mechanism capable of being reproduced in size-structured, successional models. Mortality can also be improved by comparing functional composition relationships such as correlations between wood density and "senescence" mortality as done in Figure S9. We suggest that density-dependent mortality be more rigorously tested for improved application of VDMs in ESMs.

The ZF2's data illustrated no biomass accumulation on transects that represent multiple landscape types (plateaus, valleys, and slopes) and soil types, typical for a quasi-equilibrium forest state. The VDMs use here were designed to represent generic lowland Amazonian forests that could be resolved at Earth systems scales, averaging across disturbance patches and cohorts, "stochastic" mortality, and subgrid landscape features. The VDM models predicted a larger present-day ΔAGB (1.2 Mg ha^{-1} year^{-1}) than observed. This discrepancy was due to an opposite trend in biomass growth and mortality predicted by all models, compared to observations. Mortality at the central Amazon site was higher than growth contributing to the neutral

ΔAGB, while the VDMs have growth outpacing mortality (Table 2). High mortality rates are consistent with other studies showing increased mortality with eCO_2 and a weakening biomass sink (Brienen et al., 2015; Bugmann & Bigler, 2011).

While the VDMs did not predict the present-day observed interannual variability in AGB, it was captured through annual stem mortality rates (stems $year^{-1}$; Figure S6) and is a good local-scale benchmark. For example, the forest inventory displayed large annual fluctuations in biomass gains and losses, which canceled each other over time leading to a biomass-neutral forest (a typical pattern in old-growth forests). Mortality of large trees is commonly the source of this large temporal variability in AGB, with punctuating episodic, single disturbance events occurring within a steady-state forest mosaic (Brokaw & Scheiner, 1989; Chambers et al., 2013). These observed large fluctuations support the argument for size-dependent vegetation demographics in ESMs. The VDMs predict larger variability in stem mortality and turnover rates with long-term fertilization compared to the big-leaf models (Figure S7) but notably predict different signs of responses.

4.1.2. Patterns and Uncertainties Related to Growth

Both VDMs predicted that all plants with DBH >10 cm had positive diameter growth increments. A notable result from the field inventory showed that sizeable portions of the population had no detectable diameter growth, even over periods of up to 10 years (Figure 4d). In the VDMs, trees that cannot meet their maintenance respiration and tissue turnover costs are in negative carbon balance and will draw down the carbon storage pool and trigger carbon starvation mortality, removing these trees from the population. ELM-FATES does allow users to choose the option to reduce a plant's maintenance respiration under low light conditions and when a plant's C storage is low, delaying C starvation-induced mortality. Our results suggest that the amount or timespan of cohorts sustaining near-zero C balance still needs to be investigated for tropical trees. Additionally, due to all models underestimating GPP compared to observed (Figure 3c; potentially due to less investment into canopy leafs; Figure 7a) yet predicted higher NPP, present-day 15-year biomass accumulation, and/or growth rates, we strongly suggest C assimilation, C use efficiency, and allocation of NPP needs to be further explored in models (Malhi, 2012). Field research of NPP allocation is starting to emerge (da Costa et al., 2014; del Aguila-Pasquel et al., 2014), but an understanding of how carbon partitioning within viable, surviving but nongrowing understory trees is a challenge for future studies. For example, branch turnover (being implemented in newer versions of ELM-FATES) may be important for maintaining viability in slow-growing trees (Marvin & Asner, 2016) (descriptions of modeled C allocation and growth strategies found in the supporting information, section 2c). Individual-based models (IBMs) that can simulate greater heterogeneity in plant growth dynamics have the ability to sustain trees that have short periods of zero growth rates [e.g., ZELIG-TROP, Holm et al., 2014]. This framework could alleviate the plant homogenization that occurs in cohort-based models, where all trees in a cohort experience identical conditions and growth properties are averaged across cohorts in a given size class.

4.2. Goal 2: Forest Response to Rising Atmospheric CO_2 and Model Application

We provide an illustration of how VDMs can simulate processes important at the ESM scale. The two VDM models have outputs that are similar to or improvements on performance of C-only big-leaf models while also providing finer scale demography and vital rates that can be informed by census data (e.g., Figures 4, S6, and S7). In addition the VDM results fall within the range of a larger Brazilian dataset (Figure S5). Application of VDMs within ESMs, as suggested by others (Fisher et al., 2018) appears attainable and fruitful. The introduction of soil nutrient processes in VDMs, and their spatial variation, should further improve tropical biomass predictions yet still challenging with many unknowns (Medvigy et al., 2019). Determining scales of benchmarks for evaluating specific model processes that would provide greater confidence in mechanisms determining various scales of biomass sink remains a challenge (Clark et al., 2017).

One of the most distinct differences between the classes of models is the representation of nutrient cycling and uptake, which under low availability can limit the CO_2 fertilization effect (Fleischer et al., 2019; Norby et al., 2010). In CLM5, limited N availability produced an increasingly constrained NPP over the 21st century (Figure 8a), as also seen by the slight decrease in leaf N:C and total vegetation N:C. However, the large biomass accumulation was sustained by the increase in NUE in CLM5, which can adjust leaf-level N allocation with environmental conditions (Xu et al., 2012). Tropical forests have long been hypothesized to be P limited and not N limited (Hall & Matson, 1999; Vitousek & Sanford, 1986). The

former is demonstrated by soil measurements of P availability (Vitousek et al., 2010) and strong vegetation response to P fertilization (Ellsworth et al., 2017), while the latter is confirmed by large N_2O effluxes (Silver et al., 2001), high N_2 fixation (Cleveland et al., 1999), and high dissolved N content in streams (Brookshire et al., 2012). ELMv1-ECA reproduced this hypothesis by the small increase in leaf N:C over time. It is uncertain whether N limitation in models is an appropriate surrogate for other nutrient constraints that might play a stronger role in the tropics such as P.

Both big-leaf models have vegetation N:C ratios that similarly become lower over time and thus lower potential photosynthesis, but ELMv1-ECA predicts a much lower biomass response to doubled CO_2 (21% vs. 48%), because modeled P limitation plays a critical role in the C sink at this site. Decreasing P:N ratios (Figures 8c and 8d) have been found to accelerate leaf senescence, limit plant productivity, and contribute to lower shoot biomass in developing plants (Güsewell, 2004). Therefore, it is commonly thought that including the P cycle in ecosystem models is critically important to predict P constraints on mature tropical forest carbon dynamics (Reed et al., 2015; Yang et al., 2014). This is further confirmed by Fleischer et al. (2019) who used an ensemble of 14 terrestrial ecosystem models at the same ZF2 site, reporting that P availability reduced the projections CO_2-induced C sink by ~50%, compared to models assuming no P limitation. The modeling of P availability has not been considered in any of the CMIP5 models, further stressing the need for explicit representation of the P cycle and its potential impacts on the C cycle.

Field data ZF2 and K34 also showed a large portion of C allocation to fine roots (23%) (Chambers, Tribuzy, et al., 2004; Malhi et al., 2009), indicating nutrient limitation in these P poor soils (Vitousek et al., 2010) similar to the shift to fine root allocation in the ELMv1-ECA over the 21st century when P was limiting (Figure 7b). This modeled shift to produce more fine roots to acquire P, in a system that already has an imbalance of available N compared to P, led to a modeled slight increase in N uptake (Figure 7b insert) and alleviation of leaf N limitation (indicated by the small rise in leaf N:C). In these simulations, rising atmospheric CO_2 further exacerbates P limitation (Figure 8c), leading to little CO_2 fertilization effect on forest biomass accumulation (Figure 6).

4.3. Goal 3: Processes Contributing to Biomass Sink Patterns in Response to β Effect

ED2 simulations predicted a greater increase and dominance in late successional tree species (compared to early) and larger sized trees in response to eCO_2 (Figure S8), both which have more woody biomass to store CO_2 and for long time periods (Chambers, Higuchi, et al., 2001). This pattern is consistent with observations by Stephenson et al. (2014) who found increased mass growth rates and biomass accumulation with tree size in angiosperms in Cameroon, Central and South America (via increases in a tree's total leaf area that outpace declines in productivity per unit of leaf area).

ELM-FATES, CLM5, and ELMv1-ECA all predicted an increase in biomass turnover rates and reductions in biomass pool longevities, under constant doubled CO_2 (Figure S7). This result suggests that the predicted biomass accumulation was not related to turnover but other processes (e.g., potentially shifts to woody allocation with increased NPP; or higher understory death), but these interactions need to be benchmarked. These increases in turnover rates was opposite to results reported by Walker et al. (2015) for two temperate forest sites, who showed that six out of seven models had decreasing vegetation turnover rates in response to elevated CO_2.

There have been assertions that biomass sink predictions in intact tropical forests have been overestimated, due to increased mortality rates, shifts to faster life-history strategies, and no accelerated tree-ring growth observed in long-term records (Brienen et al., 2015; van der Sleen et al., 2015). The VDMs, which are parameterized for a generic Amazon forest, predicted a large ΔAGB that was similar to older estimates based on field measurements from across the Basin (Baker et al., 2004; Lewis, 2006; Phillips et al., 1998), which have been noted to potentially have artifactual biased trends favoring growth and biomass gain (Feeley et al., 2007; Fisher et al., 2008). Instead, and similar to results of the P-enabled ELMv1-ECA model used here, Chambers and Silver (2004) concluded that a 25% increase in productivity (ELMv1-ECA predicted 23%) or a 31% increase in biomass stocks with doubling CO_2 (Wright, 2013) (ELMv1-ECA predicted 21%) may be more reasonable compared to the biomass gains in Phillips et al. (1998), Baker et al. (2004), Lewis (2006). Furthermore, CO_2 fertilization results from the subtropical EucFACE study (Ellsworth et al., 2017) showed almost no increase in productivity, mainly due to P limitation (confirmed by a paired P fertilization

experiment), consistent with only the ELMv1-ECA predictions at our ZF2 site. Clearly, the predicted and measured spread in biomass change over time in the Amazon region is highly variable, with biomass neutrality of individual sites being present but not consistent.

Both the C-only ED2 and CLM5-C simulations had large increases in woody NPP and the largest ΔAGB over 200 years, unlikely outcomes given current understanding of eCO_2 effects and constraints (Chambers & Silver, 2004; Fleischer et al., 2019; Wright, 2013). The overestimated growth increments by the VDMs warrant critical investigation into the fundamentals of NPP response to eCO_2, as well as investigating the lack of fully representing slow-growing understory and smaller DBH stems which contribute to a higher proportion of larger trees. Key processes in large trees are also ignored in these models, such as allocation to stress defenses (e.g., parasites, infection, and secondary metabolites). ELM-FATES predicted the third largest biomass sink with eCO_2 (0.80 Mg ha^{-1} $year^{-1}$), which compares to the Brazilian Amazon estimate of 0.9 Mg ha^{-1} $year^{-1}$ covering larger spatial scales (Aragão et al., 2014). Compared to ED2, this is a lower biomass response and potentially due to more accurate (i.e., lower) estimates of growth and mortality rates and the switch from calculating photosynthesis functions based on Collatz et al. (1991) in ED2 to Farquhar et al. (1980) in ELM-FATES, thus including a different temperature-dependent function, J_{max}, and including the triose-phosphate limited rate. This model-observation comparison highlights the challenge of representing tropical biomass sink dynamics in a system that may be highly variable in space and time, as well as nutrient limited.

5. Conclusions

We find that the patterns and trajectories of biomass accumulation in response to eCO_2 vary widely across six simulations from four terrestrial biosphere models due to different model structures and assumptions. With respect to the contemporary climate, mean annual net biomass increments from all models were within the field data interannual variability. Over the 15-year observational period field data show that there was no net change in biomass, whereas the models diverge from the field data and predict a continuous biomass accumulation (i.e., trends in linear coefficients and their standard errors). A wide range in present-day AGB was predicted across all model variants, contributing to varying initial AGB states thus varying projections. The challenge in representing observed interannual variability of biomass and confronting landscape-scale models with appropriate scales of observed data are important issues to resolve for future evaluation of model-derived simulations.

Three of the four models estimate that this central Amazon site will be a large biomass C sink under a doubling of CO_2 by 2100. ELMv1-ECA, which represents both dynamic allocation and C-N-P nutrient competition, predicted the lowest forest C sink over the 21st century due to P limitation (21% increase in biomass), an estimate that is closer to recent studies that do not support a large tropical C sink (Brienen et al., 2015; van der Sleen et al., 2015). This result indicates that tropical CO_2 fertilization experiments are of critical importance (Norby et al., 2016) to distinguish between likely future responses of the tropical forest C sink. The long-term β effect response by ELM-FATES was similar to the big-leaf C-only versions indicating that the future inclusion of nutrient competition in ELM-FATES, along with the detailed benefit of fine-scale demography, will help to improve eCO_2 response. We further advocate that the inclusion of ecosystem heterogeneity and demography into ESMs that account for nutrient limitations will better represent processes that govern carbon fluxes and their responses to environmental change.

Acknowledgments
This research and J. H., R. K., Q. Z., C. K., M. L., R. N., L. K., P. M., and J. C. were supported as part of the Next Generation Ecosystem Experiments-Tropics, funded by the U.S. Department of Energy, Office of Science, Office of Biological and Environmental Research under Contract DE-AC02-05CH11231. J. H., R. K., Q. Z., and W. R. were also supported as part of the Energy Exascale Earth System (E3SM) Program, as well as Laboratory Directed Research and Development (LDRD) funding from Berkeley Lab, funded by the U.S. Department of Energy, Office of Science, Office of Biological and Environmental Research. A. N. L., A. A., A. M., and N. H. were supported by the Instituto Nacional de Pesquisas da Amazônia (INPA) who also collected and led the forest inventory data collection and meteorological measurements. R. F. is funded by the National Center for Atmospheric Research, which is supported by the National Science Foundation. ML was supported by São Paulo Research Foundation (FAPESP, Grant 2015/07227-6). We also would like to thank Bardan Ghimire for his consultation regarding N cycling diagnostics in the CLM5 model. Table 2 and Figure S4 contained a portion of previously published data, for purposes of comparison to this study, which can be found via the published references listed in each caption. The field inventory dataset from the ZF2-EEST site can be accessed through the NGEE-Tropics Project after adhering to the NGEE-Tropics data policy and approval from coauthor Niro Higuchi. All the meteorological data used in this study can be found openly at the AmeriFlux site (after creating a user profile) http://ameriflux.lbl.gov/sites/siteinfo/BR-Ma2#overview. ED2 can be downloaded and available publicly at https://github.com/EDmodel/ED2. ELM-FATES can be downloaded and available publicly at https://github.com/NGEET/fates-release using the git commit "4a5d626" and the version corresponding to tag "sci.1.0.0_api.1.0.0." CLM5.0 is publicity available through the Community Terrestrial System Model (CTSM) git repository at https://github.com/ESCOMP/ctsm, using the git commit "c9868bf." ELMv1.1-ECA can be downloaded and available publicly at https://github.com/E3SM-Project/E3SM/tree/v1.1.0, using the git commit "a0bfaa8."

References

Aragão, L. E. O. C., Poulter, B., Barlow, J. B., Anderson, L. O., Malhi, Y., Saatchi, S., et al. (2014). Environmental change and the carbon balance of Amazonian forests. *Biological Reviews*, *89*(4), 913–931. https://doi.org/10.1111/brv.12088

Araújo, A. C., Nobre, A. D., Kruijt, B., Elbers, J. A., Dallarosa, R., Stefani, P., et al. (2002). Comparative measurements of carbon dioxide fluxes from two nearby towers in a central Amazonian rainforest: The Manaus LBA site. *Journal of Geophysical Research*, *107*(D20), 8090. https://doi.org/10.1029/2001jd000676

Asner, G. P. (2013). Geography of forest disturbance. *Proceedings of the National Academy of Sciences*, *110*(10), 3711–3712. https://doi.org/10.1073/pnas.1300396110

Baillie, I. (1996). Soils of the humid tropics. In P. W. Richards (Ed.), *The tropical rain forest* (pp. 256–285). Cambridge: Cambridge University Press.

Baker, T. R., Phillips, O. L., Malhi, Y., Almeida, S., Arroyo, L., di Fiore, A., et al. (2004). Increasing biomass in Amazonian forest plots. *Philosophical Transactions of the Royal Society of London. Series B: Biological Sciences*, *359*(1443), 353–365. https://doi.org/10.1098/rstb.2003.1422

Ball, J. T., Woodrow, I. E., & Berry, J. A. (1987). A model predicting stomatal conductance and its contribution to the control of photosynthesis under different environmental conditions. In J. Biggins (Ed.), *Progress in photosynthesis research* (pp. 221–224). Dordrecht: Springer. https://doi.org/10.1007/978-94-017-0519-6_48

Brienen, R. J. W., Phillips, O. L., Feldpausch, T. R., Gloor, E., Baker, T. R., Lloyd, J., et al. (2015). Long-term decline of the Amazon carbon sink. *Nature*, *519*(7543), 344–348. https://doi.org/10.1038/nature14283

Brokaw, N. V. L., & Scheiner, S. M. (1989). Species composition in gaps and structure of a tropical forest. *Ecology*, *70*(3), 538–541. https://doi.org/10.2307/1940196

Brookshire, E. N. J., Gerber, S., Menge, D. N. L., & Hedin, L. O. (2012). Large losses of inorganic nitrogen from tropical rainforests suggest a lack of nitrogen limitation. *Ecology Letters*, *15*(1), 9–16. https://doi.org/10.1111/j.1461-0248.2011.01701.x

Brzostek, E. R., Fisher, J. B., & Phillips, R. P. (2014). Modeling the carbon cost of plant nitrogen acquisition: Mycorrhizal trade-offs and multipath resistance uptake improve predictions of retranslocation. *Journal of Geophysical Research – Biogeosciences*, *119*(8), 1684–1697. https://doi.org/10.1002/2014JG002660

Bugmann, H., & Bigler, C. (2011). Will the CO_2 fertilization effect in forests be offset by reduced tree longevity? *Oecologia*, *165*(2), 533–544. https://doi.org/10.1007/s00442-010-1837-4

Cabral, O. M. R., McWilliam, A. L. C., & Roberts, J. M. (1996). *In-canopy microclimate of Amazonian forest and estimates of transpiration*. Chichester, UK: John Wiley and Sons.

Chambers, J. Q., Higuchi, N., Teixeira, L. M., dos Santos, J., Laurance, S. G., & Trumbore, S. E. (2004). Response of tree biomass and wood litter to disturbance in a central Amazon forest. *Oecologia*, *141*(4), 596–611. https://doi.org/10.1007/s00442-004-1676-2

Chambers, J. Q., Higuchi, N., Tribuzy, E. S., & Trumbore, S. E. (2001). Carbon sink for a century. *Nature*, *410*(6827), 429–429.

Chambers, J. Q., Negrón-Juarez, R. I., Marra, D. M., Di Vittorio, A., Tews, J., Roberts, D., et al. (2013). The steady-state mosaic of disturbance and succession across an old-growth central Amazon forest landscape. *Proceedings of the National Academy of Sciences*, *110*(10), 3949–3954. https://doi.org/10.1073/pnas.1202894110

Chambers, J. Q., Santos, J. D., Ribeiro, R. J., & Higuchi, N. (2001). Tree damage, allometric relationships, and above-ground net primary production in central Amazon forest. *Forest Ecology and Management*, *152*(1–3), 73–84. https://doi.org/10.1016/S0378-1127(00)00591-0

Chambers, J. Q., & Silver, W. L. (2004). Some aspects of ecophysiological and biogeochemical responses of tropical forests to atmospheric change. *Philosophical Transactions of the Royal Society of London. Series B: Biological Sciences*, *359*(1443), 463–476. https://doi.org/10.1098/rstb.2003.1424

Chambers, J. Q., Tribuzy, E. S., Toledo, L. C., Crispim, B. F., Higuchi, N., Santos, J., et al. (2004). Respiration from a tropical forest ecosystem: Partitioning of sources and low carbon use efficiency. *Ecological Applications*, *14*(sp4), 72–88. https://doi.org/10.1890/01-6012

Clark, D. A., Asao, S., Fisher, R., Reed, S., Reich, P. B., Ryan, M. G., et al. (2017). Field data to benchmark the carbon-cycle models for tropical forests. *Biogeosciences Discussions*, *2017*, 1–44. https://doi.org/10.5194/bg-2017-169

Clark, D. A., Clark, D. B., & Oberbauer, S. F. (2013). Field-quantified responses of tropical rainforest aboveground productivity to increasing CO_2 and climatic stress, 1997–2009. *Journal of Geophysical Research: Biogeosciences*, *118*(2), 783–794. https://doi.org/10.1002/jgrg.20067

Cleveland, C. C., Townsend, A. R., Schimel, D. S., Fisher, H., Howarth, R. W., Hedin, L. O., et al. (1999). Global patterns of terrestrial biological nitrogen (N2) fixation in natural ecosystems. *Global Biogeochemical Cycles*, *13*(2), 623–645. https://doi.org/10.1029/1999GB900014

Collatz, G. J., Ball, J. T., Grivet, C., & Berry, J. A. (1991). Physiological and environmental regulation of stomatal conductance, photosynthesis and transpiration: A model that includes a laminar boundary layer. *Agricultural and Forest Meteorology*, *54*(2), 107–136. https://doi.org/10.1016/0168-1923(91)90002-8

Cox, P. M., Pearson, D., Booth, B. B., Friedlingstein, P., Huntingford, C., Jones, C. D., & Luke, C. M. (2013). Sensitivity of tropical carbon to climate change constrained by carbon dioxide variability. *Nature*, *494*(7437), 341–344. https://doi.org/10.1038/nature11882

da Costa, A. C. L., Metcalfe, D. B., Doughty, C. E., de Oliveira, A. A. R., Neto, G. F. C., da Costa, M. C., et al. (2014). Ecosystem respiration and net primary productivity after 8–10 years of experimental through-fall reduction in an eastern Amazon forest. *Plant Ecology and Diversity*, *7*(1-2), 7–24. https://doi.org/10.1080/17550874.2013.798366

de Almeida Castanho, A. D., Galbraith, D., Zhang, K., Coe, M. T., Costa, M. H., & Moorcroft, P. (2016). Changing Amazon biomass and the role of atmospheric CO_2 concentration, climate, and land use. *Global Biogeochemical Cycles*, *30*(1), 18–39. https://doi.org/10.1002/2015GB005135

de Carvalho Conceição Telles, E., de Camargo, P. B., Martinelli, L. A., Trumbore, S. E., da Costa, E. S., Santos, J., & Niro Higuchi, R. C. O. Jr. (2003). Influence of soil texture on carbon dynamics and storage potential in tropical forest soils of Amazonia. *Global Biogeochemical Cycles*, *17*(2), 1040. https://doi.org/10.1029/2002GB001953

De Kauwe, M. G., Medlyn, B. E., Zaehle, S., Walker, A. P., Dietze, M. C., Wang, Y. P., et al. (2014). Where does the carbon go? A model–data intercomparison of vegetation carbon allocation and turnover processes at two temperate forest free-air CO_2 enrichment sites. *New Phytologist*, *203*(3), 883–899. https://doi.org/10.1111/nph.12847

del Aguila-Pasquel, J., Doughty, C. E., Metcalfe, D. B., Silva-Espejo, J. E., Girardin, C. A. J., Chung Gutierrez, J. A., et al. (2014). The seasonal cycle of productivity, metabolism and carbon dynamics in a wet seasonal forest in north-west Amazonia (Iquitos, Peru). *Plant Ecology and Diversity*, *7*(1-2), 71–83. https://doi.org/10.1080/17550874.2013.798365

Ellsworth, D. S., Anderson, I. C., Crous, K. Y., Cooke, J., Drake, J. E., Gherlenda, A. N., et al. (2017). Elevated CO_2 does not increase eucalypt forest productivity on a low-phosphorus soil. *Nature Climate Change*, *7*(4), 279–282. https://doi.org/10.1038/nclimate3235

Farquhar, G. D., von Caemmerer, S., & Berry, J. A. (1980). A biochemical model of photosynthetic CO_2 assimilation in leaves of C3 species. *Planta*, *149*(1), 78–90. https://doi.org/10.1007/bf00386231

Feeley, K., Wright, S. J., Muhammad Noor, N. S., Kassim, A. R., & Davies, S. J. (2007). Decelerating growth in tropical forest trees. *Ecology Letters*, *10*, 461–469. https://doi.org/10.1111/j.1461-0248.2007.01033.x

Fisher, J. B., Melton, F., Middleton, E., Hain, C., Anderson, M., Allen, R., et al. (2017). The future of evapotranspiration: Global requirements for ecosystem functioning, carbon and climate feedbacks, agricultural management, and water resources. *Water Resources Research*, *53*(4), 2618–2626. https://doi.org/10.1002/2016wr020175

Fisher, J. B., Sitch, S., Malhi, Y., Fisher, R. A., Huntingford, C., & Tan, S.-Y. (2010). Carbon cost of plant nitrogen acquisition: A mechanistic, globally applicable model of plant nitrogen uptake, retranslocation, and fixation. *Global Biogeochemical Cycles*, *24*, GB1014. https://doi.org/10.1029/2009GB003621

Fisher, J. I., Hurtt, G. C., Thomas, R. Q., & Chambers, J. Q. (2008). Clustered disturbances lead to bias in large-scale estimates based on forest sample plots. *Ecology Letters*, *11*(6), 554–563. https://doi.org/10.1111/j.1461-0248.2008.01169.x

Fisher, R. A., Koven, C. D., Anderegg, W. R. L., Christoffersen, B. O., Dietze, M. C., Farrior, C. E., et al. (2018). Vegetation demographics in Earth System Models: A review of progress and priorities. *Global Change Biology*, *24*(1), 35–54. https://doi.org/10.1111/gcb.13910

Fisher, R. A., McDowell, N., Purves, D., Moorcroft, P., Sitch, S., Cox, P., et al. (2010). Assessing uncertainties in a second-generation dynamic vegetation model caused by ecological scale limitations. *New Phytologist*, *187*(3), 666–681. https://doi.org/10.1111/j.1469-8137.2010.03340.x

Fisher, R. A., Muszala, S., Verteinstein, M., Lawrence, P., Xu, C., McDowell, N. G., et al. (2015). Taking off the training wheels: the properties of a dynamic vegetation model without climate envelopes, CLM5(ED). *Geoscientific Model Development*, *8*(11), 3593–3619. https://doi.org/10.5194/gmd-8-3593-2015

Fleischer, K., Rammig, A., Kauwe, M. G., Walker, A. P., Domingues, T. F., Fuchslueger, L., et al. (2019). Amazon forest response to CO_2 fertilization dependent on plant phosphorus acquisition. *Nature Geoscience*, *12*(9), 736–741. https://doi.org/10.1038/s41561-019-0404-9

Friedlingstein, P., Joel, G., Field, C. B., & Fung, I. Y. (1999). Toward an allocation scheme for global terrestrial carbon models. *Global Change Biology*, *5*(7), 755–770. https://doi.org/10.1046/j.1365-2486.1999.00269.x

Friedlingstein, P., Meinshausen, M., Arora, V. K., Jones, C. D., Anav, A., Liddicoat, S. K., & Knutti, R. (2014). Uncertainties in CMIP5 climate projections due to carbon cycle feedbacks. *Journal of Climate*, *27*(2), 511–526. https://doi.org/10.1175/JCLI-D-12-00579.1

Ghimire, B., Riley, W. J., Koven, C. D., Mu, M., & Randerson, J. T. (2016). Representing leaf and root physiological traits in CLM improves global carbon and nitrogen cycling predictions. *Journal of Advances in Modeling Earth Systems*, *8*(2), 598–613. https://doi.org/10.1002/2015MS000538

Güsewell, S. (2004). N:P ratios in terrestrial plants: Variation and functional significance. *New Phytologist*, *164*(2), 243–266. https://doi.org/10.1111/j.1469-8137.2004.01192.x

Hall, S. J., & Matson, P. A. (1999). Nitrogen oxide emissions after nitrogen additions in tropical forests. *Nature*, *400*(6740), 152–155.

Hoffman, F. M., Randerson, J. T., Arora, V. K., Bao, Q., Cadule, P., Ji, D., et al. (2014). Causes and implications of persistent atmospheric carbon dioxide biases in Earth System Models. *Journal of Geophysical Research: Biogeosciences*, *119*(2), 141–162. https://doi.org/10.1002/2013JG002381

Holm, J. A., Chambers, J. Q., Collins, W. D., & Higuchi, N. (2014). Forest response to increased disturbance in the central Amazon and comparison to western Amazonian forests. *Biogeosciences*, *11*(20), 5773–5794. https://doi.org/10.5194/bg-11-5773-2014

Huntingford, C., Zelazowski P., Galbraith D., Mercado L. M., Sitch S., Fisher R., et al. (2013). Simulated resilience of tropical rainforests to CO_2-induced climate change. *Nature Geoscience*, *6*, 268. https://doi.org/10.1038/ngeo1741, https://www.nature.com/articles/ngeo1741

IPCC (2000). Special report: emission scenarios Rep., 570 pp, Cambridge, UK.

Keller, K. M., Lienert, S., Bozbiyik, A., Stocker, T. F., Churakova (Sidorova), O. V., Frank, D. C., et al. (2017). 20th century changes in carbon isotopes and water-use efficiency: Tree-ring-based evaluation of the CLM5 and LPX-Bern models. *Biogeosciences*, *14*(10), 2641–2673. https://doi.org/10.5194/bg-14-2641-2017

Kennedy, D., Swenson, S., Oleson, K. W., Lawrence, D. M., Fisher, R., Lola da Costa, A. C., & Gentine, P. (2019). Implementing plant hydraulics in the community land model, Version 5. *Journal of Advances in Modeling Earth Systems*, *11*(2), 485–513. https://doi.org/10.1029/2018ms001500

King, D. A., Davies, S. J., & Noor, N. S. M. (2006). Growth and mortality are related to adult tree size in a Malaysian mixed dipterocarp forest. *Forest Ecology and Management*, *223*(1– 3), 152–158. https://doi.org/10.1016/j.foreco.2005.10.066

Knox, R. G. (2012). Land conversion in Amazonia and Northern South America; influences on regional hydrology and ecosystem response, Dissertation thesis, Massachusetts Institute of Technology, Cambridge, MA.

Knox, R. G., Longo, M., Swann, A. L. S., Zhang, K., Levine, N. M., Moorcroft, P. R., & Bras, R. L. (2015). Hydrometeorological effects of historical land-conversion in an ecosystem-atmosphere model of Northern South America. *Hydrology and Earth System Sciences*, *19*(1), 241–273. https://doi.org/10.5194/hess-19-241-2015

Körner, C. (2003). Slow in, rapid out—Carbon flux studies and Kyoto targets. *Science*, *300*(5623), 1242–1243. https://doi.org/10.1126/science.1084460

Koven, C. D., Riley, W. J., Subin, Z. M., Tang, J. Y., Torn, M. S., Collins, W. D., et al. (2013). The effect of vertically resolved soil biogeochemistry and alternate soil C and N models on C dynamics of CLM4. *Biogeosciences*, *10*(11), 7109–7131. https://doi.org/10.5194/bg-10-7109-2013

Lamarque, J. F., Bond, T. C., Eyring, V., Granier, C., Heil, A., Klimont, Z., et al. (2010). Historical (1850–2000) gridded anthropogenic and biomass burning emissions of reactive gases and aerosols: Methodology and application. *Atmospheric Chemistry and Physics*, *10*(15), 7017–7039. https://doi.org/10.5194/acp-10-7017-2010

Lawrence, D. M., Fisher, R. A., Koven, C. D., Oleson, K. W., Swenson, S. C., Bonan, G., et al. (2019). The Community Land Model version 5: Description of new features, benchmarking, and impact of forcing uncertainty. *Journal of Advances in Modeling Earth Systems*, *11*(12), 4245–4287. https://doi.org/10.1029/2018MS001583

Levine, N. M., Zhang, K., Longo, M., Baccini, A., Phillips, O. L., Lewis, S. L., et al. (2016). Ecosystem heterogeneity determines the ecological resilience of the Amazon to climate change. *Proceedings of the National Academy of Sciences*, *113*(3), 793–797. https://doi.org/10.1073/pnas.1511344112

Lewis, S. L. (2006). Tropical forests and the changing earth system. *Philosophical Transactions of the Royal Society, B: Biological Sciences*, *361*(1465), 195–210. https://doi.org/10.1098/rstb.2005.1711

Lewis, S. L., Lopez-Gonzalez, G., Sonké, B., Affum-Baffoe, K., Baker, T. R., Ojo, L. O., et al. (2009). Increasing carbon storage in intact African tropical forests. *Nature*, *457*(7232), 1003–1006. https://doi.org/10.1038/nature07771

Longo, M. (2014). Amazon forest response to changes in rainfall regime: Results from an individual-based dynamic vegetation model, Doctoral dissertation thesis, Harvard University.

Longo, M., Knox, R. G., Levine, N. M., Swann, A. L. S., Medvigy, D. M., Dietze, M. C., et al. (2019). The biophysics, ecology, and biogeochemistry of functionally diverse, vertically- and horizontally-heterogeneous ecosystems: The Ecosystem Demography Model, version 2.2—Part 2: Model evaluation. *Geoscientific Model Development Discussion*, *2019*, 1–34. https://doi.org/10.5194/gmd-2019-71

Luo, Y., Hui, D., & Zhang, D. (2006). Elevated CO_2 stimulates net accumulations of carbon and nitrogen in land ecosystems: A meta-analysis. *Ecology*, *87*(1), 53–63. https://doi.org/10.1890/04-1724

Luo, Y., Su, B., Currie, W. S., Dukes, J. S., Finzi, A., Hartwig, U., et al. (2004). Progressive nitrogen limitation of ecosystem responses to rising atmospheric carbon dioxide. *Bioscience*, *54*(8), 731–739. https://doi.org/10.1641/0006-3568(2004)054[0731:PNLOER]2.0.CO;2

Malhi, Y. (2012). The productivity, metabolism and carbon cycle of tropical forest vegetation. *Journal of Ecology*, *100*(1), 65–75.

Malhi, Y., Aragao, L. E. O. C., Metcalfe, D., Paiva, R., Quesada, C. A., Almeida, S., et al. (2009). Comprehensive assessment of carbon productivity, allocation and storage in three Amazonian forests. *Global Change Biology*, *15*(5), 1255–1274. https://doi.org/10.1111/j.1365-2486.2008.01780.x

Manokaran, N., & Kochummen, K. M. (1987). Recruitment, growth and mortality of tree species in a lowland dipterocarp forest in Peninsular Malaysia. *Journal of Tropical Ecology*, *3*(4), 315–330. https://doi.org/10.1017/S0266467400002303

Marvin, D. C., & Asner, G. P. (2016). Branchfall dominates annual carbon flux across lowland Amazonian forests. *Environmental Research Letters*, *11*(9), 094027.

McDowell, N., Allen, C. D., Anderson-Teixeira, K., Brando, P., Brienen, R., Chambers, J., et al. (2018). Drivers and mechanisms of tree mortality in moist tropical forests. *New Phytologist*, *219*(3), 851–869. https://doi.org/10.1111/nph.15027

McGuire, A. D., Melillo, A. J. M., & Joyce, L. A. (1995). The role of nitrogen in the response of forest net primary production to elevated atmospheric carbon dioxide. *Annual Review of Ecology and Systematics*, *26*(1), 473–503. https://doi.org/10.1146/annurev.es.26.110195.002353

Medlyn, B. E., Badeck, F. . W., de Pury, D. G. G., Barton, C. V. M., Broadmeadow, M., Ceulemans, R., et al. (1999). Effects of elevated [CO_2] on photosynthesis in European forest species: A meta-analysis of model parameters. *Plant, Cell & Environment*, *22*(12), 1475–1495. https://doi.org/10.1046/j.1365-3040.1999.00523.x

Medlyn, B. E., de Kauwe, M. G., Zaehle, S., Walker, A. P., Duursma, R. A., Luus, K., et al. (2016). Using models to guide field experiments: A priori predictions for the CO_2 response of a nutrient- and water-limited native Eucalypt woodland. *Global Change Biology*, *22*(8), 2834–2851. https://doi.org/10.1111/gcb.13268

Medlyn, B. E., Duursma, R. A., Eamus, D., Ellsworth, D. S., Prentice, I. C., Barton, C. V. M., et al. (2011). Reconciling the optimal and empirical approaches to modelling stomatal conductance. *Global Change Biology*, *17*(6), 2134–2144. https://doi.org/10.1111/j.1365-2486.2010.02375.x

Medlyn, B. E., Zaehle, S., de Kauwe, M. G., Walker, A. P., Dietze, M. C., Hanson, P. J., et al. (2015). Using ecosystem experiments to improve vegetation models. *Nature Climate Change*, *5*(6), 528–534. https://doi.org/10.1038/nclimate2621

Medvigy, D., Wang, G., Zhu, Q., Riley, W. J., Trierweiler, A. M., Waring, B. G., et al. (2019). Observed variation in soil properties can drive large variation in modelled forest functioning and composition during tropical forest secondary succession. *New Phytologist*, *223*(4), 1820–1833. https://doi.org/10.1111/nph.15848

Medvigy, D., Wofsy, S. C., Munger, J. W., Hollinger, D. Y., & Moorcroft, P. R. (2009). Mechanistic scaling of ecosystem function and dynamics in space and time: Ecosystem Demography model version 2. *Journal of Geophysical Research*, *114*, G01002. https://doi.org/10.1029/2008JG000812

Medvigy, D., Wofsy, S. C., Munger, J. W., & Moorcroft, P. R. (2010). Responses of terrestrial ecosystems and carbon budgets to current and future environmental variability. *Proceedings of the National Academy of Sciences*, *107*(18), 8275–8280. https://doi.org/10.1073/pnas.0912032107

Mercado, L. M., Huntingford, C., Gash, J. H. C., Cox, P. M., & Jogireddy, V. (2007). Improving the representation of radiation interception and photosynthesis for climate model applications. *Tellus B*, *59*(3), 553–565. https://doi.org/10.1111/j.1600-0889.2007.00256.x

Moorcroft, P. R., Hurtt, G. C., & Pacala, S. W. (2001). A method for scaling vegetation dynamics: The ecosystem demography model (ED). *Ecological Monographs*, *71*(4), 557–586. https://doi.org/10.1890/0012-9615(2001)071[0557:AMFSVD]2.0.CO;2

Negrón-Juárez, R. I., Koven, C. D., Riley, W. J., Knox, R. G., & Chambers, J. Q. (2015). Observed allocations of productivity and biomass, and turnover times in tropical forests are not accurately represented in CMIP5 Earth system models. *Environmental Research Letters*, *10*(6), 064017.

Niu, J., Shen, C., Chambers, J. Q., Melack, J. M., & Riley, W. J. (2017). Interannual variation in hydrologic budgets in an Amazonian watershed with a coupled subsurface—Land surface process model. *Journal of Hydrometeorology*. https://doi.org/10.1175/jhm-d-17-0108.1

Norby, R. J., de Kauwe, M. G., Domingues, T. F., Duursma, R. A., Ellsworth, D. S., Goll, D. S., et al. (2016). Model–data synthesis for the next generation of forest free-air CO_2 enrichment (FACE) experiments. *New Phytologist*, *209*(1), 17–28. https://doi.org/10.1111/nph.13593

Norby, R. J., Warren, J. M., Iversen, C. M., Medlyn, B. E., & McMurtrie, R. E. (2010). CO_2 enhancement of forest productivity constrained by limited nitrogen availability. *Proceedings of the National Academy of Sciences*, *107*(45), 19,368–19,373. https://doi.org/10.1073/pnas.1006463107

Oleson, K. W., D.M. Lawrence, G.B. Bonan, B. Drewniak, M. Huang, C.D. Koven, et al. (2013). Technical Description of version 4.5 of the Community Land Model (CLM). Ncar Technical Note NCAR/TN-503 + STR Rep., 422 pp, National Center for Atmospheric Research, Boulder, CO.

Pan, Y., Birdsey, R. A., Fang, J., Houghton, R., Kauppi, P. E., Kurz, W. A., et al. (2011). A large and persistent carbon sink in the world's forests. *Science*, *333*(6045), 988–993. https://doi.org/10.1126/science.1201609

Phillips, O. L., Lewis, S. L., Baker, T. R., Chao, K.-J., & Higuchi, N. (2008). The changing Amazon forest. *Philosophical Transactions of the Royal Society, B: Biological Sciences*, *363*(1498), 1819–1827. https://doi.org/10.1098/rstb.2007.0033

Phillips, O. L., Malhi, Y., Higuchi, N., Laurance, W. F., Nunez, P. V., Vasquez, R. M., et al. (1998). changes in the carbon balance of tropical forests: Evidence from long-term plots. *Science*, *282*(5388), 439–442. https://doi.org/10.1126/science.282.5388.439

Purves, D. W., Lichstein, J. W., Strigul, N., & Pacala, S. W. (2008). Predicting and understanding forest dynamics using a simple tractable model. *Proceedings of the National Academy of Sciences*, *105*(44), 17,018–17,022. https://doi.org/10.1073/pnas.0807754105

Purves, D. W., & Pacala, S. W. (2008). Predictive models of forest dynamics. *Science*, *320*(5882), 1452–1453. https://doi.org/10.1126/science.1155359

Quesada, C. A., Lloyd, J., Schwarz, M., Patiño, S., Baker, T. R., Czimczik, C., et al. (2010). Variations in chemical and physical properties of Amazon forest soils in relation to their genesis. *Biogeosciences*, *7*(5), 1515–1541. https://doi.org/10.5194/bg-7-1515-2010

Rammig, A., Tim, J., Kirsten, T., Britta, T., Jens, H., Sebastian, O., et al. (2010). Estimating the risk of Amazonian forest dieback. *New Phytologist*, *187*(3), 694–706. https://doi.org/10.1111/j.1469-8137.2010.03318.x

Reed, S. C., Yang, X., & Thornton, P. E. (2015). Incorporating phosphorus cycling into global modeling efforts: A worthwhile, tractable endeavor. *New Phytologist*, *208*(2), 324–329. https://doi.org/10.1111/nph.13521

Restrepo-Coupe, N., da Rocha, H. R., Hutyra, L. R., da Araujo, A. C., Borma, L. S., Christoffersen, B., et al. (2013). What drives the seasonality of photosynthesis across the Amazon basin? A cross-site analysis of eddy flux tower measurements from the Brasil flux network. *Agricultural and Forest Meteorology*, *182-183*, 128–144. https://doi.org/10.1016/j.agrformet.2013.04.031

Riley, W. J., Zhu, Q., & Tang, J. Y. (2018). Weaker land–climate feedbacks from nutrient uptake during photosynthesis-inactive periods. *Nature Climate Change*, *8*(11), 1002–1006. https://doi.org/10.1038/s41558-018-0325-4

Shi, X., Mao, J., Thornton, P. E., & Huang, M. (2013). Spatiotemporal patterns of evapotranspiration in response to multiple environmental factors simulated by the Community Land Model. *Environmental Research Letters*, *8*, 024012.

Silver, W. L., Herman, D. J., & Firestone, M. K. (2001). Dissimilatory nitrate reduction to ammonium in upland tropical forest soils. *Ecology*, *82*(9), 2410–2416. https://doi.org/10.1890/0012-9658(2001)082[2410:DNRTAI]2.0.CO;2

Silver, W. L., & Miya, R. K. (2001). Global patterns in root decomposition: Comparisons of climate and litter quality effects. *Oecologia*, *129*(3), 407–419. https://doi.org/10.1007/s004420100740

Stephenson, N. L., Das, A. J., Condit, R., Russo, S. E., Baker, P. J., Beckman, N. G., et al. (2014). Rate of tree carbon accumulation increases continuously with tree size. *Nature*, *507*(7490), 90–93. https://doi.org/10.1038/nature12914

Sitch, S., Friedlingstein, P., Gruber, N., Jones, S. D., Murray-Tortarolo, G., Ahlström, A., et al. (2015). Recent trends and drivers of regional sources and sinks of carbon dioxide. *Biogeosciences*, *12*(3), 653–679. https://doi.org/10.5194/bg-12-653-2015

Tang, J. Y., & Riley, W. J. (2013). A total quasi-steady-state formulation of substrate uptake kinetics in complex networks and an example application to microbial litter decomposition. *Biogeosciences*, *10*(12), 8329–8351. https://doi.org/10.5194/bg-10-8329-2013

Tang, Z., Xu, W., Zhou, G., Bai, Y., Li, J., Tang, X., et al. (2018). Patterns of plant carbon, nitrogen, and phosphorus concentration in relation to productivity in China's terrestrial ecosystems. *Proceedings of the National Academy of Sciences*, *115*(16), 4033–4038. https://doi.org/10.1073/pnas.1700295114

Taylor, K. E., Stouffer, R. J., & Meehl, G. A. (2012). An overview of CMIP5 and the experiment design. *Bulletin of the American Meteorological Society*, *93*(4), 485–498. https://doi.org/10.1175/BAMS-D-11-00094.1

Thompson, M. V., Randerson, J. T., Malmström, C. M., & Field, C. B. (1996). Change in net primary production and heterotrophic respiration: How much is necessary to sustain the terrestrial carbon sink? *Global Biogeochemical Cycles*, *10*(4), 711–726. https://doi.org/10.1029/96GB01667

van der Sleen, P., Groenendijk, P., Vlam, M., Anten, N. P. R., Boom, A., Bongers, F., et al. (2015). No growth stimulation of tropical trees by 150 years of CO_2 fertilization but water-use efficiency increased. *Nature Geoscience*, *8*(1), 24–28. https://doi.org/10.1038/ngeo2313

Vitousek, P. M., Porder, S., Houlton, B. Z., & Chadwick, O. A. (2010). Terrestrial phosphorus limitation: Mechanisms, implications, and nitrogen–phosphorus interactions. *Ecological Applications*, *20*(1), 5–15. https://doi.org/10.1890/08-0127.1

Vitousek, P. M., & Sanford, R. L. (1986). Nutrient cycling in moist tropical forest. *Annual Review of Ecology and Systematics*, *17*, 137–167.

Vogt, K. A., Vogt, D. J., Palmiotto, P. A., Boon, P., O'Hara, J., & Asbjornsen, H. (1995). Review of root dynamics in forest ecosystems grouped by climate, climatic forest type and species. *Plant and Soil*, *187*(2), 159–219. https://doi.org/10.1007/bf00017088

Walker, A. P., Beckerman, A. P., Gu, L., Kattge, J., Cernusak, L. A., Domingues, T. F., et al. (2014). The relationship of leaf photosynthetic traits—V_{cmax} and J_{max}—to leaf nitrogen, leaf phosphorus, and specific leaf area: A meta-analysis and modeling study. *Ecology and Evolution*, *4*(16), 3218–3235. https://doi.org/10.1002/ece3.1173

Walker, A. P., Zaehle, S., Medlyn, B. E., de Kauwe, M. G., Asao, S., Hickler, T., et al. (2015). Predicting long-term carbon sequestration in response to CO_2 enrichment: How and why do current ecosystem models differ? *Global Biogeochemical Cycles*, *29*(4), 476–495. https://doi.org/10.1002/2014GB004995

Wang, R., Balkanski, Y., Boucher, O., Ciais, P., Peñuelas, J., & Tao, S. (2015). Significant contribution of combustion-related emissions to the atmospheric phosphorus budget. *Nature Geoscience*, *8*, 48. https://doi.org/10.1038/ngeo2324, https://www.nature.com/articles/ngeo2324

Wang, Y. P., Houlton, B. Z., & Field, C. B. (2007). A model of biogeochemical cycles of carbon, nitrogen, and phosphorus including symbiotic nitrogen fixation and phosphatase production. *Global Biogeochemical Cycles*, *21*, GB1018. https://doi.org/10.1029/2006GB002797

Wehr, R., Commane, R., Munger, J. W., McManus, J. B., Nelson, D. D., Zahniser, M. S., et al. (2017). Dynamics of canopy stomatal conductance, transpiration, and evaporation in a temperate deciduous forest, validated by carbonyl sulfide uptake. *Biogeosciences*, *14*(2), 389–401. https://doi.org/10.5194/bg-14-389-2017

Wieder, W. R., Lawrence, D. M., Fisher, R. A., Bonan, G. B., Cheng, S. J., Goodale, C. L., et al. (2019). Beyond static benchmarking: Using experimental manipulations to evaluate land model assumptions. *Global Biogeochemical Cycles*, *33*(10), 1289–1309. https://doi.org/10.1029/2018gb006141

Wright, J. S. (2013). The carbon sink in intact tropical forests. *Global Change Biology*, *19*(2), 337–339. https://doi.org/10.1111/gcb.12052

Xu, C., Fisher, R., Wullschleger, S. D., Wilson, C. J., Cai, M., & McDowell, N. G. (2012). Toward a mechanistic modeling of nitrogen limitation on vegetation dynamics. *PLoS ONE*, *7*(5), e37914. https://doi.org/10.1371/journal.pone.0037914

Yang, X., Post, W. M., Thornton, P. E., & Jain, A. (2013). The distribution of soil phosphorus for global biogeochemical modeling. *Biogeosciences*, *10*(4), 2525–2537. https://doi.org/10.5194/bg-10-2525-2013

Yang, X., Thornton, P. E., Ricciuto, D. M., & Post, W. M. (2014). The role of phosphorus dynamics in tropical forests—A modeling study using CLM-CNP. *Biogeosciences*, *11*(6), 1667–1681. https://doi.org/10.5194/bg-11-1667-2014

Zaehle, S., Medlyn, B. E., de Kauwe, M. G., Walker, A. P., Dietze, M. C., Hickler, T., et al. (2014). Evaluation of 11 terrestrial carbon–nitrogen cycle models against observations from two temperate Free-Air CO_2 Enrichment studies. *New Phytologist*, *202*(3), 803–822. https://doi.org/10.1111/nph.12697

Zhang, K., de Almeida Castanho, A. D., Galbraith, D. R., Moghim, S., Levine, N. M., Bras, R. L., et al. (2015). The fate of Amazonian ecosystems over the coming century arising from changes in climate, atmospheric CO_2, and land use. *Global Change Biology*, *21*(7), 2569–2587. https://doi.org/10.1111/gcb.12903

Zhang, K., Kimball, J. S., Zhao, M., Oechel, W. C., Cassano, J., & Running, S. W. (2007). Sensitivity of pan-Arctic terrestrial net primary productivity simulations to daily surface meteorology from NCEP-NCAR and ERA-40 reanalyses. *Journal of Geophysical Research*, *112*, G01011. https://doi.org/10.1029/2006JG000249

Zhu, Q., & Riley, W. J. (2015). Improved modelling of soil nitrogen losses. *Nature Climate Change*, *5*(8), 705–706. https://doi.org/10.1038/nclimate2696

Zhu, Q., Riley, W. J., & Tang, J. (2017). A new theory of plant–microbe nutrient competition resolves inconsistencies between observations and model predictions. *Ecological Applications*, *27*(3), 875–886. https://doi.org/10.1002/eap.1490

Zhu, Q., Riley, W. J., Tang, J., & Koven, C. D. (2016). Multiple soil nutrient competition between plants, microbes, and mineral surfaces: Model development, parameterization, and example applications in several tropical forests. *Biogeosciences*, *13*(1), 341–363. https://doi.org/10.5194/bg-13-341-2016